Journal of Electronics and Electrical Engineering
https://ojs.wiserpub.com/index.php/JEEE

Review

Advancements and Challenges in Microstrip Dual-Band Bandpass Filters: A Comprehensive Survey

Tarun Kumar Das[1*], Sayan Chatterjee[2], Bhaskar Gupta[2]

[1] Department of Electronics and Communication Engineering, Future Institute of Engineering and Management, Kolkata, India
[2] Department of Electronics and Telecommunication Engineering, Jadavpur University, Kolkata, India
[*] Correspondence: tarunj1979@gmail.com

Received: 17 April 2026; **Revised:** 18 June 2026; **Accepted:** 23 June 2026; **Published:** 17 July 2026

Abstract: The growing demand for multi-frequency wireless communication systems has significantly increased research interest in multi-band radio frequency (RF) and microwave filters. Designing multi-band RF and microwave filters that are efficient, affordable, compact, lightweight, and easy to fabricate presents a significant challenge. Multi-band bandpass filters (BPFs), including dual-, tri-, and quad-band variants, are pivotal in simplifying RF systems by reducing component count, particularly in multi-band transceivers. Creating compact and efficient dual-band filters is essential for modern electronic devices operating in dual frequency bands. This article presents a thorough analysis of prior research on microstrip dual-band bandpass filter designs, emphasizing current developments and the challenges encountered. A detailed comparison of several design strategies is provided and discussed to offer researchers insights into the benefits and drawbacks of each technique for specific applications. This article also outlines the challenges and future research directions for dual-band microstrip BPFs to meet various performance goals in current and future wireless systems.

Keywords: dual-band bandpass filter, compactness, harmonics suppression, microstrip, review, selectivity, wireless systems

1. Introduction

Dual-band bandpass filters exhibit remarkable versatility, seamlessly facilitating the transmission of two distinct frequency bands while effectively suppressing interference from unwanted frequencies, offering unparalleled signal clarity in wireless communication systems. With applications spanning from modern Wi-Fi routers including IEEE 802.16, 802.11, GSM, CDMA, etc. [1] to advanced radar systems, dual-band bandpass filters emerge as indispensable components, enabling efficient spectrum utilization by selectively transmitting signals in two predetermined frequency ranges while mitigating adjacent channel interference. Depending on the particular integration process, these filters can be implemented using various techniques, such as lumped-element filters, distributed-element filters, by using various planar and non-planar transmission lines. The first miniaturized monolithic dual-band filter for dual-mode portable telephones was proposed in [2], using a ceramic lamination technique. This approach involves stacking multiple ceramic layers with precise geometrical configurations to create a compact filter capable of selectively passing two distinct frequency bands. Since then, interest in dual-band filters has increased greatly during the past two decades, and a lot of research has been carried out extensively. In designing dual-band bandpass filters, the researchers have faced several challenges, including: (1) maintaining sufficient

Copyright ©2026 Tarun Kumar Das, et al.
DOI: https://doi.org/10.37256/jeee.52202610029
This is an open-access article distributed under a CC BY license
(Creative Commons Attribution 4.0 International License)
https://creativecommons.org/licenses/by/4.0/

isolation between the two intended passbands while reducing crosstalk and interference, especially for closely separated passbands, (2) obtaining exact control over both passband bandwidths to satisfy the demands of individual frequency bands without compromising the filter's overall performance, (3) maintaining minimal insertion loss in each passband to guarantee effective signal transmission in both frequency bands and reduce signal attenuation, (4) ensuring high return loss for the effective impedance matching and low signal reflection at the input and output ports, confirming ideal power transfer and lower signal loss, (5) providing high stopband rejection to reduce signals outside of the passbands, such as harmonics, spurious emissions, and interference from nearby frequency bands, (6) ensuring that components like resonators, capacitors, and inductors are properly matched in order to minimize variances in insertion loss and return loss, (7) designing tiny and compact filters that prevent electromagnetic interference (EMI) and preserve optimal performance, particularly for space-constrained applications, (8) taking into account thermal impacts and temperature fluctuations to guarantee consistent performance across a broad working temperature range, (9) ensuring reliable and cost-effective manufacturing while maintaining high yield rates, considering factors such as component tolerances, fabrication processes, and material characteristics, (10) ensuring frequency tunability or reconfigurability to adapt changing operational requirements or frequency allocation regulations, and (11) controlling the fluctuations in phase and group delay in both passbands, especially in communication and radio frequency (RF) front-end applications, to prevent distortion and preserve signal integrity.

To tackle such design constraints, various methods and materials have been studied by the researchers based on the required specifications of the dual-band filters for different applications, as demonstrated in Table 1. The detail description of some of the application areas of Table 1 is elaborated as follows:

• **Wi-Fi (2.4/5 GHz, 5% FBW):** Dual-band filters in Wi-Fi routers and access points must simultaneously support the 2.4 GHz (IEEE 802.11b/g/n) and 5 GHz (IEEE 802.11a/n/ac) bands. The 5% fractional bandwidth requirement reflects the moderate selectivity needed to coexist with other nearby ISM-band signals [3].

• **GSM/UMTS (900/2100 MHz, 3%–8% FBW):** Compact dual-band filters are necessary for GSM and UMTS networks, which frequently run at 900 MHz and 2100 MHz, in order to accommodate both current data services and legacy telephony within a single RF front-end [4].

• **5G NR (3.5/28 GHz, 5%–10% FBW):** For 5G New Radio base stations and user equipment, dual-band filters must bridge the sub-6 GHz (FR1) and millimeter-wave (FR2) bands. The significant frequency ratio (approximately 8:1) between these bands makes this one of the most challenging dual-band filter design scenarios and directly motivates several works reviewed in this survey [5].

• **Satellite Communication (4/12 GHz):** C-band uplink (5.925–6.425 GHz) and downlink (3.7–4.2 GHz) for traditional geostationary satellites, combined with Ku-band (10.7–12.75 GHz) for direct broadcast and VSAT, create a classical dual-band filtering requirement [6].

• **Automotive Radar (24/77 GHz, 5%–10% FBW):** Short-range radar (24 GHz) and long-range radar (77 GHz) are both used in ADAS systems, requiring dual-band filters capable of operating at both mmWave frequencies simultaneously. The extreme frequency ratio and mmWave operational requirements make this a frontier application for microstrip dual-band filter research [7].

• **IoT/WSN (868/2400 MHz or 915/2450 MHz, 2%–10% FBW):** Wireless Sensor Network (WSN) [8] and Internet of Things (IoT) [9] devices often use 2.4 GHz for high-data-rate communication and sub-GHz bands for long-range connectivity. In resource-constrained sensor nodes, dual-band filters minimize size, power consumption, and electromagnetic interference while enabling smooth multi-band operation.

• **Military Communication (L-/S-Band, 5%–15% FBW):** Multiple frequency bands are used by contemporary military communication systems to provide safe, dependable, and jam-resistant transmission. In challenging electromagnetic conditions, dual-band filters maintain high selectivity, resilience, and spectrum efficiency while enabling simultaneous operation across tactical and strategic communication channels [10].

• **Medical Implantable Devices (0.4/2.4 GHz, 5%–10% FBW):** Implantable devices such as pacemakers, cochlear implants, and neurostimulators use the MICS band (402–405 MHz) for close-range telemetry and the ISM band (2.4 GHz) for higher-speed data transfer. Dual-band filters in this domain must also satisfy stringent size and biocompatibility constraints [11].

• **Drone Communication (2.4/5.8 GHz, 5%–10% FBW):** Unmanned aerial vehicles (UAVs) often employ 5.8 GHz for high-definition video transmission and 2.4 GHz for command-and-control communications. Effective channel isolation, interference reduction, and lightweight RF front-ends appropriate for aerial platforms all require compact dual-band filters [12].

• **Space-Based Communication (S-/X-Band or Ku-/Ka-Band, 2%–8% FBW):** For telemetry, tracking, command, and payload data transfer, satellite and space communication systems frequently use a variety of frequency bands. Dual-band filters guarantee great durability, low insertion loss, and steady operation under harsh environmental conditions while assisting in the reduction of payload size and weight [13].

• **Smart Home (2.4/5 GHz, 5%–15% FBW):** Dual-band Wi-Fi networks that operate at 2.4 GHz and 5 GHz are essential to smart home ecosystems. Compact and affordable wireless modules with better coexistence, less interference, and increased connectivity for networked smart devices are made possible by dual-band filters [14].

Table 1. Applications of dual-band bandpass filters

Area	f_{o1}/f_{o2} (GHz)	3-dB *FBW* (%)	Applications
Wi-Fi	2.4/5	5/5	Wi-Fi routers, access points [3]
GSM	0.9/1.8	As per the requirements of the cellular network	Cellular base stations, mobile devices, and infrastructure supporting GSM and UMTS [4]
UMTS	1.9/2.1		
5G NR	3.5/28	5–10	5G base stations, small cells, and User Equipment (UE) [5]
Satellite Communication	4/12	vary based on standards and requirements	Satellite ground stations, satellite communication terminals, and satellite modems [6]
Automotive Radar	24/77	5–10	Advanced Driver Assistance Systems (ADAS) and autonomous vehicles for radar sensing applications such as adaptive cruise control, collision avoidance, and blind spot detection [7]
Internet of Things (IoT)	0.868/2.4	vary based on specific protocols and applications	Devices and sensors operating for long-range communication and local area connectivity [9]
Military Communication	1/10	configurable based on requirements	Tactical radios, satellite terminals, and electronic warfare (EW) systems [10]
Medical Implantable Devices	0.4/2.4	5–10	Implantable medical devices like pacemakers and neuro-stimulators [11]
Drone Communication	2.4/5.8	5–10	unmanned aerial vehicles (UAVs) or drones for various purposes including aerial photography, surveillance, mapping, and delivery [12]
Industrial Wireless Sensor Networks (WSN)	0.868/2.4	vary based on specific IoT protocols and applications	Industrial automation and monitoring systems utilizing WSN for collecting data from sensors and actuators [8]
Space-Based Communication	2/8	configurable based on specific satellite communication standards and applications	broadcasting, broadband internet access, remote sensing, and scientific missions [13]
Smart Home	2.4/5 for Wi-Fi, 0.9 for Zigbee 0.9/2.4 for Z-Wave	5–10	Home automation systems, smart thermostats, security cameras, and other IoT devices [14]

Popular methodologies for designing dual-band bandpass filters include (1) frequency transformation method [8, 15–27], (2) coupled resonator-based designs [28–65], (3) multi-mode resonator-based designs [5, 66–109], (4) fractal-based designs [110–119], (5) defected ground structures (DGS)-based designs [120–132] and metamaterial-based tunable filter designs [133–141]. All such techniques provide various methodologies to create microstrip dual-band bandpass filters, each with pros and cons of their own. The specifications of the filters, such as frequency ranges, bandwidths, size restrictions, and manufacturing technologies, are some of the elements that influence the approach choice. However, two types of studies have been carried out for all techniques: some of them are primarily focused on the compactness of the filters' sizes and the improvement of the passband characteristics, such as low insertion loss, high return loss, good isolation between the

passbands, and high skirt selectivity, and others have exhibited superior stopband rejection in addition to the improvement of the passbands characteristics and compactness. In the subsequent sections, all such studies are reviewed, along with their novelties and limitations. Finally, the present article ends with a summary in the conclusion section, highlighting the effectiveness of dual-band filters for modern wireless communication systems.

2. Frequency transformation method

To create a prototype filter with the appropriate frequency characteristics, the frequency transformation method (FTM) is employed in filter design. Such an approach has also been used to design dual-band filters. There are six successive steps to be followed in this method: (1) determining the filter order and transfer function such as Butterworth, Chebyshev, or Elliptic type compliance with predetermined criteria; (2) designing a prototype filter with the desired frequency response characteristics for a single bandpass filter; (3) synthesizing the network and coupling matrix; (4) scaling and shifting the frequency axis of the prototype filter to match the desired passbands of the dual-band filter; (5) adjusting the separation between the passbands by manipulating the parameters of the prototype filter, and (6) physically realizing the filter to ensure that it meets the desired specifications for both passbands, including characteristics such as bandwidth, insertion loss, return loss, and stopband attenuation. The pioneering filter design within this category was introduced in reference [15], tailored specifically for GSM mobile communication systems. Later, many dual-band filters were designed, as reported in [8, 16–27]. For all such filters, high selectivity (110–330 dB/GHz), good isolation of passbands (30–50 dB), low insertion loss (0.2–1.04 dB), and high return loss (18–23 dB) were obtained. In addition, a good upper stopband rejection level (30–50 dB) has also been reported for some of the filters. For instance, in [20], by utilizing the out-of-phase property of two back-to-back E-shaped resonators, a wide stopband with a rejection level of 50 dB up to $2.35f_{01}$ was obtained, where f_{01} is the center frequency of the first passband of the dual-band filter. However, the size of the filter in [20] is quite large. Later, in [22] (Figure 1), a modified Richard's transformation (MRT) has been introduced for designing asymmetrical-response dual-band bandpass filters with a compact size of $0.04\lambda_g \times 0.54\lambda_g$ (λ_g is the guided wavelength at the center frequency of the first passband), allowing independent adjustment of bandwidths and center frequencies through the use of eighth-wavelength transmission lines. Such a novel approach enhances filter performance and simplifies the design process, making it particularly beneficial for various communication applications. Meanwhile, in [23], the stopband becomes wider up to $3.55f_{01}$ with a poor rejection level of only 15 dB due to the employment of three-section coupled lines and three short-circuit stubs in the filter's structure. Table 2 explores the performance of some of these proposed filters based on certain parameters.

It has been revealed from Table 2 that the filter in [22] has exhibited the best performance concerning the compact size, middle stopband rejection level, upper stopband rejection level, and upper stopband rejection bandwidth. The design of such types of filters has several advantages, such as: (1) they provide more flexibility and efficiency for the designers to utilize the theoretical and practical knowledge of the existing Butterworth, Chebyshev, and elliptic prototype filter designs [16]; (2) by properly scaling and adjusting the prototype filter's frequency response, designers can adjust the dual-band filter's passband features, such as bandwidth, center frequency, and shape factor [17–19]; and (3) they provide ease of implementation and integration with other components [19–23]. However, such filters also suffer from a few limitations, such as (1) limited frequency range (500 MHz to 6 GHz); (2) poor sensitivity to transformation parameters [16, 17]; (3) achieving desired characteristics in both passbands, trade-offs in other performance parameters, such as insertion loss, return loss, and stopband attenuation, may require with increase design iterations [19, 20]; (4) for non-standard criteria, such as stringent specifications on passband ripple or stopband attenuation, the complexity of the design process may increase and additional techniques or adjustments may be needed [8, 23, 24]; (5) high dependency on the characteristics of the prototype filter, restricting wide varieties of applications [25], and (6) the sizes of the filters are quite large due to the use of straight resonators [20, 22, 23, 27]. Subsequently, the researchers investigated coupled resonator-based designs as an alternative, as discussed in the next section.

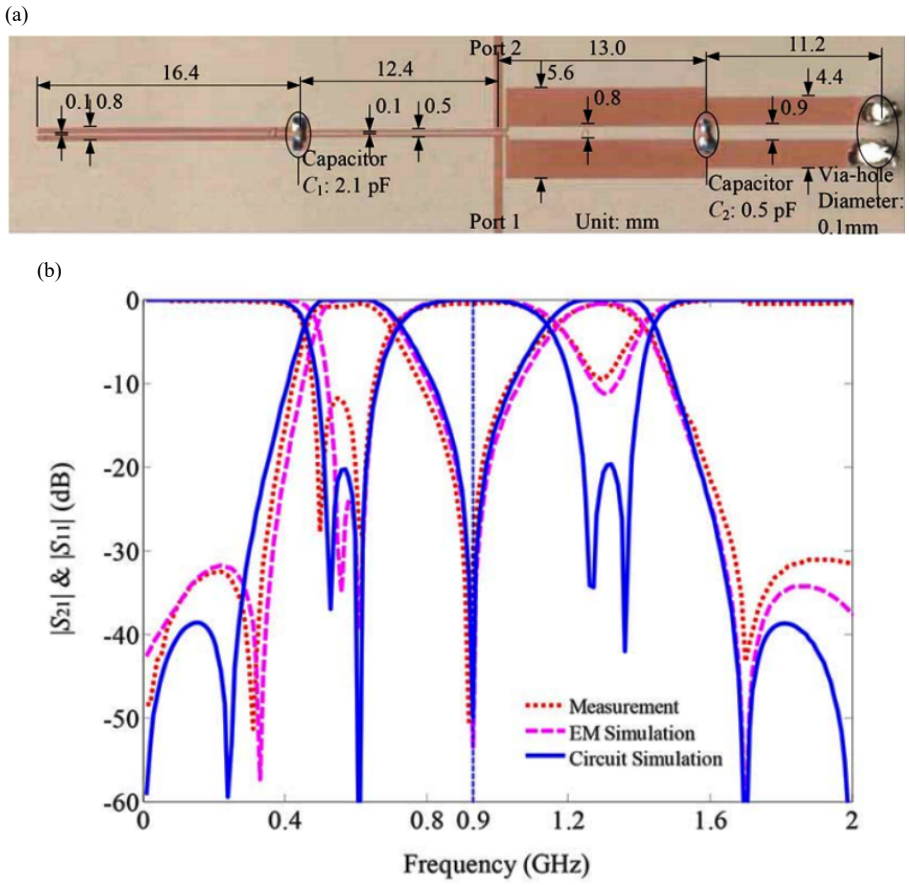

Figure 1. (a) Photograph of the fabricated filter with dimensions labeled; (b) Frequency responses of the theoretical, simulated and measured results [22]

Table 2. Comparative study of dual-band bandpass filters based on frequency transformation method (FTM)

Ref. no.	f_{o1}/f_{o2} (GHz)	*FBW* (%)	*IL* (dB)	*RL* (dB)	*MSRL* (dB)	*TZs*	Size $\lambda_g \times \lambda_g$	*USBRL* (dB)	*USBW* ($\times f_{o1}$)	Substrate specifications		
										ε_r	*h* (mm)	tan δ
[18]	3.93/4.08	2.5/2.5	4.0/4.5	12/13	>32	3	0.36 × 0.12	>30	1.15	2.2	1.574	0.0009
[20]	1.63/2.28	9.2/6.6	0.9/1.2	18/16	>40	2	0.84 × 0.70	>50	2.35	10.2	0.635	0.0021
[22]	0.58/1.31	39.6/18.3	0.3/0.9	21/23	>50	1	0.04 × 0.54	>30	3.45	10.8	0.635	0.0023
[23]	0.705/1.37	41.1/19	0.55/1.04	13/15	>22	3	0.33 × 0.05	>15	3.55	3.66	0.762	0.0037
[26]	2.4/2.6	3.2/3.2	2.05/2.46	20/20	>23	2	0.23 × 0.15	>40	1.67	2.2	0.508	0.0009
[27]	0.50/2.0	41.2/56	0.2/0/7	10/11	>20	3	0.11 × 0.13	>10	6.0	2.65	2.0	0.003

In Table 2, f_{01} and f_{02} = center frequencies of the passbands, 3-dB *FBW* = fractional bandwidth, *IL* = Insertion loss, *RL* = Return loss, *MSRL* = Middle stopband rejection level, *TZs* = no. of transmission zeros between two passbands,

USBRL = Upper stopband rejection level, *USBW* = Upper stopband width, ε_r = Dielectric constant, h = thickness and $\tan\delta$ = loss tangent of the substrate material, NR: Not reported in the article (same for all tables).

3. Coupled resonators based designs

Coupled resonator structures are employed to create dual-band passbands with controlled bandwidths and frequency separation. This method is based on the following steps: (1) defining specifications of the filter, (2) selecting the appropriate filter topology such as parallel-coupled resonators, cross-coupled resonators, or a combination of both, (3) calculating resonator parameters such as resonant frequency, coupling coefficient, and quality factor (Q-factor), (4) optimizing performance metrics of the filter by performing EM simulation, and (5) finally, fabricating the prototype filter to measure different parameters of the filters as per the specifications. In general, two types of resonators are utilized in this type of dual-band filter design such as parallel-coupled and cross-coupled resonators.

3.1 *Parallel-coupled resonators (PCR) based filters*

Two types of configurations have been studied by the researchers for the design of these types of dual-band filters by cascading (1) uniform parallel-coupled resonators and (2) stepped impedance-coupled resonators in an appropriate arrangement. The first filter in category 1 was proposed in [28], where a double-transmission-line resonator consisting of two open-ended edge-coupled half-wavelength transmission-line segments has been employed. Although the proposed filter exhibits good isolation between the passbands (more than 32 dB), the size of the filter is quite large ($1.1\lambda_g \times 0.28\lambda_g$), and the contribution of such a resonator to the suppression of spurious harmonics is not studied in [28]. Accordingly, both the passband and stopband characteristics of the dual-band filters have been investigated in [29, 30] by proposing different coupling configurations of the parallel resonators. For instance, in [29], coupled-line and coupled three-line resonators are employed to obtain a wide stopband up to $4.3f_{01}$ with a rejection level of 28.9 dB. A split-type dual-band filter with quarter-wavelength hook-type coupled-resonators is designed in [30] to obtain a stopband up to $2.8f_{01}$ with a moderate attenuation level of 28 dB. However, both the filters in [29, 30] have quite large sizes, restricting their applications in modern wireless systems.

As an alternative method, stepped-impedance parallel-coupled lines have been employed by different researchers. Basically, a stepped-impedance resonator (SIR) is made up of several portions of a transmission line with different impedances. Resonant behavior at particular frequencies results from reflections and standing waves created during the transition between these sections. SIRs are very popular in dual-band filters and impedance-matching networks. Due to their inherent built-in dual-band functioning, fast frequency responses, compactness, design flexibility, enhanced selectivity, reduced losses, simplicity of integration, and wideband capabilities, SIRs are appropriate for a broad range of dual-band filtering applications [31]. They provide improved discrimination between desirable and undesired frequencies, low insertion losses, and precise control over center frequencies and bandwidths.

In this context, compact-sized dual-band filters with high selectivity and good isolation between passbands have been proposed in [32–40] by employing coupled SIRs. The lengths and widths of different sections of the SIRs have been tuned optimally to achieve the desired characteristics of the filters. However, for all such filters, the effects of the SIRs on the spurious harmonics have not been focused on. Additionally, filters designed in [36, 38, 40], exhibit considerably large dimensions, and thereby impose limitations on their practical applications. Subsequently, a group of researchers has investigated both the passband and stopband performances of the dual-band filters based on SIRs.

In [41] a dual-band filter with compact size ($0.48\lambda_g \times 0.09\lambda_g$), enhanced selectivity (370 dB/GHz) at the lower edge and 62.5 dB/GHz at the upper edge), well-isolated passbands (more than 42 dB), and wide out-of-band rejection ($8.3f_{01}$ with a rejection level of 30 dB) have been explored by utilizing stepped-impedance resonators with varying dimensions (Figure 2). However, the sizes of the filters are quite large for [41–43, 45, 46] ($0.67\lambda_g \times 0.32\lambda_g$) except for the filter proposed in [44] ($0.45\lambda_g \times 0.32\lambda_g$). Although the filter proposed in [44] is compact in size, the rejection level of the spurious harmonics is only 20 dB and is extended up to $3.27f_{01}$. Table 3 highlights the comparative study of some of the best filters proposed in this category to validate the effectiveness of parallel-coupled SIRs. It has been observed that the filter in

[41] has exhibited the best performance. However, for dual-band bandpass filters, parallel-coupled stepped-impedance resonators (SIRs) pose difficulties. These include the inability to achieve desirable features due to cross-coupling effects [41], increased insertion losses (3.45–2.67 dB), complexity in fabrication [45], sensitivity to manufacturing changes [46], and restricted tunability of the bandwidth [47]. Sophisticated design methods and careful thoughts are required to overcome these obstacles and guarantee the best possible filter performance.

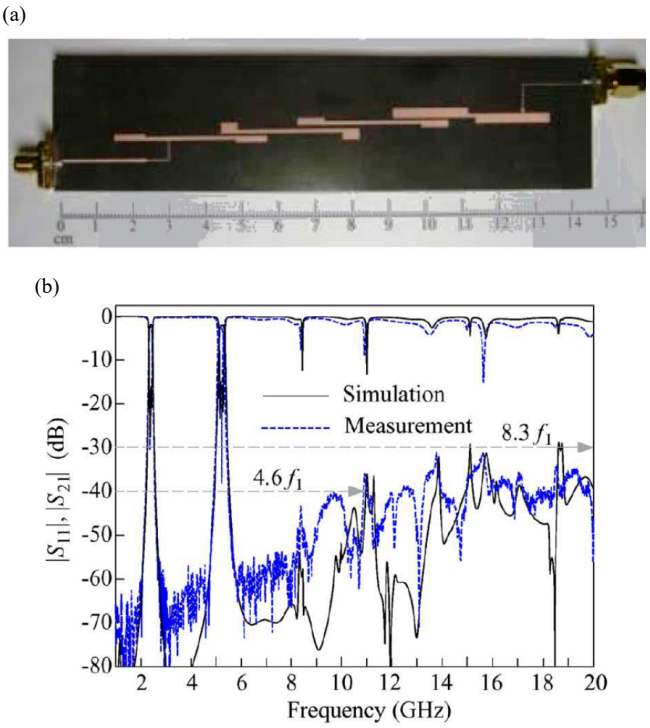

Figure 2. (a) Photograph of the fabricated filter with dimensions labeled; (b) Frequency responses of the simulated and measured results [41]

Table 3. Comparative study of dual-band bandpass filters based on parallel-coupled UIRs and SIRs based

Ref. no.	f_{o1}/f_{o2} (GHz)	3-dB FBW (%)	IL (dB)	RL (dB)	$MSRL$ (dB)	TZs	Size $\lambda_g \times \lambda_g$	$USBRL$ (dB)	$USBW$ ($\times f_{o1}$)	Substrate specifications		
										ε_r	h (mm)	$\tan\delta$
[28]	1.15/1.43	7.83/4.9	1.52/2.52	14/9.7	>32	2	1.1 × 0.28	>50	1.85	9.8	1.19	0.0025
[29]	0.9/1.575	38/37	0.99/1.32	22/23	>30	1	NR	>28.9	3.97	10.2	1.27	0.0023
[30]	1.8/2.45	5/5	1.13/1.17	26/28	>32	2	0.14 × 0.35	>28	2.5	10.8	1.27	0.002
[34]	1.6/2.45	4.5/5.5	1.46/1.16	12/12	>55	1	0.22 × 0.21	>25	2.06	6.15	0.635	0.0027
[35]	2.4/5.2	10.3/6	2.27/2.88	8.88/9	>40	2	NR	>31	3.625	6.15	0.635	0.0027
[36]	2.65/7.85	62/18	0.2/0.4	20/14	>65	1	0.22 × 0.18	20	3.77	6.15	1.27	0.0027
[38]	2.45/3.42	3.7/1.5	1.02/3.01	17/18	>40	1	0.17 × 0.18	35	1.63	2.55	0.787	0.002
[39]	2.33/4.36	6/5.7	2.0/2.2	16/17	>28	2	0.28 × 0.23	>38	2.58	3.66	0.508	0.0027

Table 3. (cont.)

Ref. no.	f_{o1}/f_{o2} (GHz)	3-dB FBW (%)	IL (dB)	RL (dB)	$MSRL$ (dB)	TZs	Size $\lambda_g \times \lambda_g$	$USBRL$ (dB)	$USBW$ ($\times f_{o1}$)	Substrate specifications		
										ε_r	h (mm)	$\tan\delta$
[41]	2.4/5.2	6/4	2.49/2.79	16/17	>60	1	0.18 × 0.16	>30	8.3	2.2	0.508	0.0009
[43]	0.9/2.49	3.6/2.1	2.67/4.65	18/17	>40	3	0.67 × 0.32	>35	5.56	3.38	0.812	0.0027
[44]	2.49/3.49	15.6/8	1.2/1.2	12/12	>35	1	0.45 × 0.32	>20	3.21	3	0.76	0.0013
[45]	2.24/4.02	17.6/9.7	2.45/2.1	11/12	>57	1	0.38 × 0.36	>21	4.24	10.2	0.635	0.0023
[46]	2.4/4	8/39	1.4/1.0	30/11	>30	1	0.48 × 0.09	>25	8.33	2.2	0.787	0.0009

3.2 *Cross-coupled resonators (CCR) based filters*

Dual-band bandpass filters featuring cross-coupled resonators emerge as integral components within microwave and radio frequency systems, playing a pivotal role in their functionality. They are made up of resonators that are tuned to particular frequency ranges and are coupled to produce transmission zeros, which increase selectivity. These filters have low insertion loss (0.2 dB) and strong selectivity (450 dB/GHz) [47] within each of the two separate frequency ranges in which they operate. Resonator frequencies, coupling coefficients, and optimization for targeted performance metrics are among the design factors to take into account. These filters are used in a variety of wireless communication systems, such as software-defined radios (SDRs), frequency division duplexing (FDD) systems, and multi-band antennas, when it is required to process signals in multiple frequency bands simultaneously. In this context, a four-pole cross-coupled dual-band microstrip bandpass filter was proposed first in [47]. Subsequently, different cross-coupled resonators-based dual-band filters have been investigated in [48–61]. Folded stepped-impedance resonators have been employed in [48–50, 52–58] to improve skirt selectivity (470 dB/GHz) and isolation between the passbands (more than 48 dB). In addition, the size of the filters becomes compact due to the cross-coupled configuration ($0.1\lambda_g \times 0.2\lambda_g$).

As an alternative approach, stub-loaded open-loop resonators have been placed in a cross-coupled structure in [51] to design a compact dual-band filter with a wide 40 dB isolation level between the two desired passbands (2.45/5.25 GHz). However, the insertion losses (2.6 dB and 3.5 dB) and return losses (12 dB and 13 dB) are not satisfactory, as reported in [51]. However, for all such filters, the main focus of investigation was the improvement of the in-band performances and size reduction. The out-of-band performances have not been reported. Subsequently, in [59–64], different modified cross-coupled resonators have been utilized in different orientations to obtain the suppression of spurious harmonics along with improved in-band performances and compact sizes. For instance, a pair of L-shaped half-wavelength SIRs and an inverted Z-shape with a pair of quarter-wavelength SIRs has been embedded in [59]. Later, spurline-embedded cross-coupled resonators were employed in [60]. For both filters, the stopband bandwidth beyond the second passband becomes more than 3.5 times the first center frequency. However, the rejection levels are restricted to 20 dB only. Subsequently, an improved upper stopband rejection level of 38 dB up to $4.18f_{01}$ has been achieved in [61] by folded SIRs, and those of 30 dB up to $4.18f_{01}$ have been reported in [62] using branch-line resonators. However, the size of the filter is quite large in [62] over [61], and the design process is complex. Subsequently, multiple transmission zeros have been generated in the stopband in [63, 64] by combining source-load cross-coupling and in [65] by employing two pairs of short-ended resonators and semi-circular trisection stepped impedance resonators (SIRs) loaded by a trapezoidal stub (Figure 3). All such filters have a broad stopband width ($3.75f_{01}$–$4.2f_{01}$ and), low 3 dB bandwidths (2.1% and 3.2%), sharp roll-off rates (450–480 dB/GHz) in the two bands, large return losses (15–30 dB), low insertion losses (0.54–1.3 dB), and compact sizes ($0.2\lambda_g \times 0.2\lambda_g$)). Table 4 highlights the comparative study of some of the best filters proposed in this category to validate the effectiveness of cross-coupled SIRs. It has been explored that the filter in [65] has exhibited the best

performance. Cross-coupled resonator-based dual-band filters suffer from some limitations, such as a larger footprint due to cross-coupled resonators (four in [60]) resulting more complex circuitry, limited out-of-band rejection level (30 dB), limited bandwidth tunability (4%–15%), higher insertion loss (more than 1.5 dB) due to increased cross-couplings, and sensitivity to fabrication tolerances. However, continuous improvements in manufacturing and design processes are carried out by different researchers to enhance the usefulness of this category of filters. Accordingly, an alternate topology based on multi-mode resonators has been reviewed in the next section.

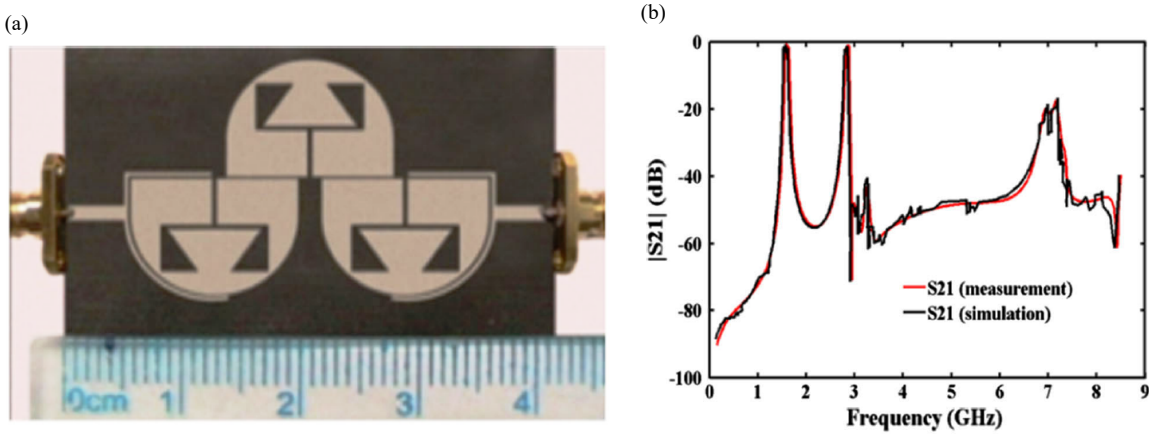

Figure 3. (a) Photograph of the fabricated filter with dimensions labeled; (b) Frequency responses of the simulated and measured results [65]

Table 4. Comparative study of dual-band bandpass filters based on cross-coupled resonators based

Ref. no.	f_{o1}/f_{o2} (GHz)	3-dB *FBW* (%)	*IL* (dB)	*RL* (dB)	*MSRL* (dB)	*TZs*	Size $\lambda_g \times \lambda_g$	*USBRL* (dB)	*USBW* ($\times f_{o1}$)	Substrate specifications		
										ε_r	*h* (mm)	tan δ
[49]	2.35/3.15	4/3	1.8/3.0	25/30	>45	1	0.18 × 0.16	>22	1.91	2.65	1.0	0.002
[52]	2.4/5.2	5/3.2	1.9/2.3	25/25	>40	1	0.16 × 0.19	>23	3.33	2.2	0.787	0.0009
[53]	2.4/5.4	7.9/3.15	1.7/2.7	12/11	>28	1	0.46 × 0.2	>42	2.92	2.2	0.787	0.0009
[54]	2.43/5.23	3.3/3.8	1.5/1.9	15/15	>22	2	0.66 × 0.16	>28	2.8	3.38	0.762	0.0027
[55]	1.66/1.92	5.1/2.8	0.75/1.48	20/22	>50	1	0.46 × 0.22	>20	4.22	2.65	1.0	0.002
[56]	1.5/3.5	11.7/9.8	0.92/1.2	19/20	>30	3	0.1 × 0.12	>20	4.3	10.2	0.635	0.0023
[57]	2.43/5.47	15.3/12.4	1.0/1.1	11/13	>38	2	0.4 × 0.19	>20	2.67	10.2	1.27	0.0023
[59]	2.45/5.2	7.7/6.09	2.26/2.23	35/38	>42	2	0.2 × 0.22	>20	1.67	10.2	0.635	0.0023
[60]	2.45/5.25	12.6/7.6	1.6/1.8	25/28	>35	2	0.49 × 0.13	>28	2.4	10.2	0.635	0.0023
[61]	1.575/2.4	6/4	0.9/1.1	30/20	>55	1	0.5 × 0.35	>38	3.37	2.2	0.787	0.0009
[62]	2.4/5.2	8/8	2.6/2.68	26/16	>38	2	0.4 × 0.31	>29	4.17	3.55	0.508	0.0027
[63]	2.45/5.25	4/8	1.3/0.8	13/22	>25	3	0.39 × 0.18	>20	4.2	2.55	0.8	0.0029
[64]	2.42/5.8	5.8/3.28	1.3/1.7	30/16	>30	4	0.2 × 0.2	>20	3.75	2.2	0.508	0.0009
[65]	1.57/2.7	3.17/2.09	0.54/0.8	22/25	>58	1	0.39 × 0.26	>40	4.27	6.15	0.79	0.0009

4. Multi-mode resonators based designs

Structures that enable the simultaneous propagation of two or more resonant modes, each with a resonance frequency that is unrelated harmonically, are known as multi-mode resonators (MMRs). Using multi-mode resonators in dual-band bandpass filters has several benefits. Compact filter designs are made possible by these resonators, which also simplify the overall structure and improve selectivity. They are ideal for many RF and microwave applications because of their adaptable frequency tuning, enhanced band isolation, and decreased complexity, all of which enhance system efficiency and performance [66]. Mainly, three types of multi-mode resonators are investigated to design dual-band filters, such as resonators with perturbation, stepped impedance resonators, and stub-loaded resonators.

4.1 *Dual-mode resonators with perturbation*

Dual-bandpass filter design relies heavily on dual-mode resonators (DMRs). Dual-mode resonators facilitate the propagation of two degenerate modes with the same resonant frequency but orthogonal field distributions. DMRs can establish distinct passbands for various frequencies by carefully designing and fine-tuning them. Coupling elements offer control over passband properties by connecting numerous DMRs to build the filter. Overall, DMRs provide a flexible foundation for the construction of dual-bandpass filters that are appropriate for a variety of RF/microwave and wireless communication applications due to their small size, excellent performance, and customizable properties. In this context, a variety of filters have been proposed in [66–74] by the researchers based on DMRs with perturbation. For instance, a dual-mode square patch resonator with a cross-shaped perturbation has been utilized in [66]. However, the proposed filter suffers from poor selectivity (220 dB/GHz for the first passband and 170 dB/GHz for the second passband), and a large size (14.2 mm $\times$ 14.2 mm). As a solution, an improved ring resonator with periodic loading of open-circuited stubs is utilized in [67, 68] to design a dual-band filter (Figure 4) with compact size (a size reduction of 22%) and adjustable spacing between the two passbands (more than 4 GHz with isolation level of 50 dB). Subsequently, the selectivity of the dual-band filter has been improved (470 dB/GHz) in [69] by embedding two slits in a square patch of similar structure as the previous design. Later, a stub-loaded patch resonator and a capacitance-loaded square loop resonator are employed in [70] and [71], respectively, to improve the selectivity (more than 400 dB/GHz) and isolation between the desired passbands (more than 45 dB). However, the size of the filter proposed in [71] is quite large (830 mm^2). As an alternative structure, a single-slotted circular patch resonator has been proposed in [72], which exhibits a sharp out-of-band rejection skirt (475 dB/GHz) and good rejection between the dual passbands (more than 22 dB) for a dual-band bandpass filter. Subsequently, a compact and highly selective dual-band filter has been proposed in [73] by employing a square loop with folded arms and mitered bends. In addition, the isolation between the two passbands has been improved by connecting the open-circuited stubs to the end of the feed lines (more than 25 dB).

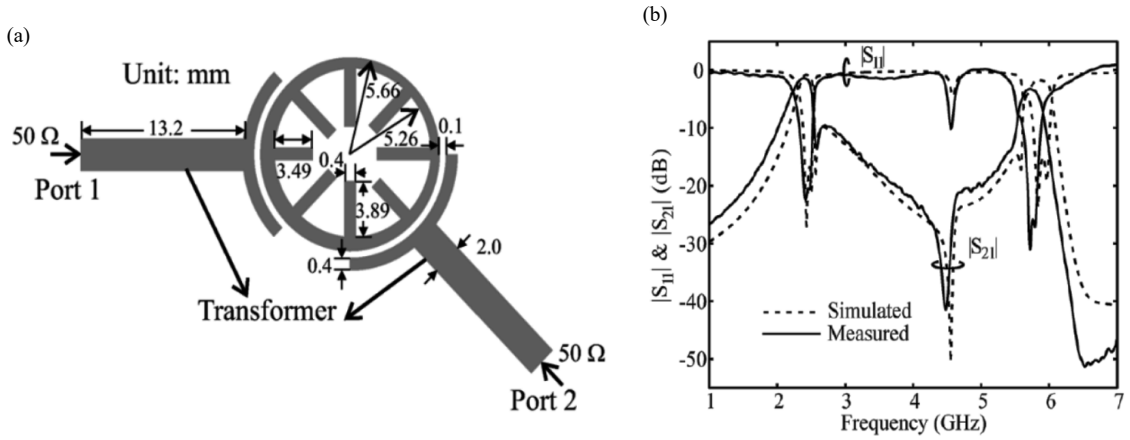

Figure 4. (a) Layout of the proposed filter with dimensions labeled; (b) Frequency responses of the simulated and measured results [67]

Such a study has been extended in [74] further by utilizing a dual-mode meandered loop resonator with internally located square loop loading elements. For all such filters of [66–74], the main research issues are compactness ($0.3\lambda_g \times 0.3\lambda_g$), enhancement of skirt selectivity (more than 400 dB/GHz), and improving the isolation between the passbands (more than 20 dB). However, the ability of spurious harmonic suppression by the structures has not been addressed. Accordingly, upper-stopband rejection levels of 26 dB and 15 dB up to $3.17f_{01}$ and $5.17f_{01}$ have been reported in [75] and [76], respectively, by loading open-circuited stubs in a square loop and by source/load coupling in a ring-loaded resonator. In addition, the size of the filter in [76] has a very compact size of $0.1\lambda_g \times 0.11\lambda_g$. Table 5 highlights the comparative study of some of the best filters reported by dual-mode resonators with perturbation. It has been revealed that the filter in [67] has exhibited the best performance. In summary, dual-mode resonator (DMR)-based dual-band bandpass filters with perturbation offer advantages like compactness ($0.1\lambda_g \times 0.11\lambda_g$), large isolation level between the passbands (more than 30 dB), and enhanced upper stopband bandwidth (more than $3f_{01}$) with an improved rejection level of 40 dB. However, they also come with several limitations, such as limited bandwidth (5% to 12%), complexity in design due to the need for precise perturbations and coupling adjustments [76], sensitivity to fabrication tolerances [73], cross-coupling effects between resonant modes [74], challenges in achieving sufficient frequency separation between dual passbands, sensitivity to temperature variations, impact stability, size constraints imposed by resonator structures [66], and perturbation elements. Despite these limitations, DMR-based filters are valuable in specific applications, requiring careful consideration during design and implementation.

Table 5. Comparative study of dual-band bandpass filters based on dual-mode resonators with perturbation

Ref. no.	f_{o1}/f_{o2} (GHz)	3-dB *FBW* (%)	*IL* (dB)	*RL* (dB)	*MSRL* (dB)	*TZs*	Size $\lambda_g \times \lambda_g$	*USBRL* (dB)	*USBW* ($\times f_{o1}$)	Substrate specifications		
										ε_r	*h* (mm)	$\tan\delta$
[67]	2.4/5.8	12/12	1.4/3.2	20/28	>10	2	0.33 × 0.15	>50	2.92	10.8	1.27	0.002
[69]	2.21/2.81	10.4/8.2	1.1/1.6	15/14	>60	1	0.31 × 0.31	>40	1.81	10.2	1.27	0.0023
[70]	2.4/5.2	13.7/6.3	0.6/1.4	28/12	>10	2	0.46 × 0.42	>10	2.33	10.2	1.27	0.0023
[72]	2.43/3.73	4.5/6.1	2.5/1.3	27/22	>18	3	0.21 × 0.22	>8	1.85	10.8	1.27	0.002
[73]	1.23/1.9	4.4/5.2	3.2/2.8	14/19	>20	2	0.12 × 0.15	>15	1.95	6.15	1.27	0.0027
[75]	2.3/4.1	12/15	0.65/1.0	24/21	>33	2	0.23 × 0.12	>26	3.17	10.8	1.27	0.002
[76]	2.4/5.2	10.6/13.5	0.36/1.0	17/22	>25	2	0.10 × 0.11	>15	5	3.5	0.508	0.0018

4.2 *Dual-mode resonators with SIRs*

The combination of dual-band functionality, compact size, design flexibility, low insertion loss, high selectivity, and ease of fabrication makes dual-mode dual-band bandpass filters with stepped-impedance resonators a desirable choice for various RF and microwave applications. In this context, different SIR structures have been investigated in [5, 77–87] to design dual-mode dual-band filters with compact size ($0.14\lambda_g \times 0.16\lambda_g$), high selectivity (480 dB/GHz), enhanced isolation between passbands (more than 52 dB), and low insertion loss (0.2 dB). For instance, pseudo-interdigital SIRs and meandering SIRs have been employed in [77] and [78], respectively. However, the isolation between the passbands was poor in [78] (less than 38 dB) compared to [77] (more than 40 dB). Accordingly, a single short-stub-loaded stepped-impedance resonator (SIR) has been utilized in [80] to improve the skirt selectivity (465 dB/GHz) and isolation between the passbands (more than 32 dB) of the dual-band filter and achieve compact size (720 mm^2). As an alternative structure, two quarter-wavelength SIRs with a common short-ended stub have been employed in [84] to design a very compact

dual-band filter ($0.14\lambda_g \times 0.16\lambda_g$). However, the skirt selectivity for both passbands becomes poor with such a structure (320 dB/GHz and 290 dB/GHz). Accordingly, a compact ($0.3\lambda_g \times 0.3\lambda_g$) filter has been proposed in [85] based on a dual-mode stepped impedance resonator (SIR). However, the skirt selectivity of the second passband (220 dB/GHz) is not good compared to that of the first passband (410 dB/GHz).

Subsequently, the selectivity improvement has been achieved significantly in [86] (415 dB/GHz) by folding SIRs with shorted coupled lines. Later, folded interlocked SIRs were employed in [5] to improve the selectivity (470 dB/GHz) of the dual-band filter applicable for 5G new radio access technologies. However, the size of the proposed filter is quite large ($0.24\lambda_g \times 0.25\lambda_g$). Accordingly, size reduction ($0.25\lambda_g \times 0.12\lambda_g$) has been achieved in [87] by employing a pair of coupled SIRs and a pair of half-wavelength bent resonators. It has been revealed from [5, 77–87] that most of the filters are compact in size ($0.14\lambda_g \times 0.16\lambda_g$), have enhanced selectivity (480 dB/GHz), and have well-isolated passbands with a high attenuation level (more than 52 dB). However, the upper out-of-band performances of the filters are unaddressed. In connection with this, both the passband and stopband performances have been investigated in [61, 88–91].

For instance, an average rejection level of 38 dB up to $3.37f_{01}$ has been reported in [61] in addition to enhanced selectivity and good isolation between the passbands using asymmetric stepped-impedance resonators (SIRs) (Figure 5). Afterward, the upper stopband width has been extended up to $5.42f_{01}$ in [89] by two open-loop SIRs. However, the rejection level is limited to only 15.5 dB. Subsequently, a very compact (size of $0.07\lambda_g \times 0.09\lambda_g$) dual-band filter with good selectivity (492 dB/GHz) along with a wide upper stopband ($4.08f_{01}$) and a good rejection level of 32 dB, has been proposed in [90]. However, the isolation level between the passbands is not so attractive (less than 25 dB). Table 6 highlights the comparative study of some of the best filters reported by dual-mode resonators with SIRs. It has been explored that the filter in [61] has exhibited the best performance. In summary, dual-mode bandpass filters with SIRs offer a compact (size of $0.07\lambda_g \times 0.09\lambda_g$, [90]) and versatile solution for achieving dual-band functionality in RF and microwave systems. However, they come with several limitations, such as limited bandwidth (4% to 25%) due to the inherent narrow bandwidth of SIRs, complex design processes requiring careful optimization of resonator dimensions and impedance ratios, sensitivity to fabrication tolerances, cross-coupling effects between resonant modes that may degrade filter performance, challenges in achieving sufficient frequency separation between dual passbands (more than 30 dB), possible compromise in insertion loss performance (more than 2 dB) compared to single-band filters, size constraints imposed by resonator structures, and the need for adequate coupling.

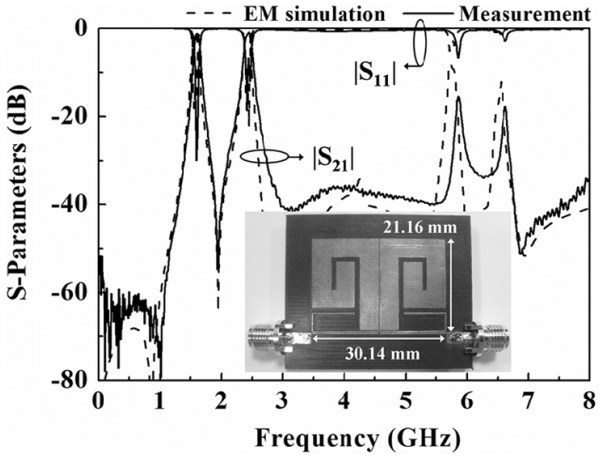

Figure 5. Photograph of the fabricated filter with dimensions labeled (inset figure) and frequency responses of the simulated and measured results [61]

Table 6. Comparative study of dual-band bandpass filters based on dual-mode resonators with SIRs

Ref. no.	f_{o1}/f_{o2} (GHz)	3-dB *FBW* (%)	*IL* (dB)	*RL* (dB)	*MSRL* (dB)	*TZs*	Size $\lambda_g \times \lambda_g$	*USBRL* (dB)	*USBW* ($\times f_{o1}$)	Substrate specifications		
										ε_r	h (mm)	$\tan\delta$
[77]	2.4/5.2	24/14	0.42/0.7	7/32	>40	1	0.22 × 0.11	>27	2.92	6.15	0.635	0.0019
[78]	2.4/5.7	10/15	1.2/1.8	19/16	>38	1	0.30 × 0.30	>12	2.5	2.55	0.8	0.001
[79]	2.35/5.05	16.6/13.5	1.64/2.91	18/12	>52	3	0.88 × 0.43	>20	2.98	9.2	1.0	0.002
[81]	1.68/2.99	3.27/2.85	1.0/1.0	22/22	>25	1	0.73 × 0.56	>35	4.76	9.2	1.0	0.002
[82]	3.88/5.35	12.4/8.6	0.38/1.03	24/19	>20	1	0.73 × 0.56	>17	1.8	1.84	0.2	0.0004
[83]	2.4/3.5	4.1/1.4	1.8/2.9	20/22	>17	2	0.67 × 0.34	>25	1.67	6.15	0.63	0.0023
[84]	0.9/1.75	42/15	0.2/0.5	18/25	>30	1	0.14 × 0.16	>15	3	3.38	0.508	0.0027
[86]	1.57/3.7	4.5/4	2.5/2.3	12/15	>15	2	0.35 × 0.40	>35	2.87	2.65	0.5	0.003
[5]	0.95/1.47	12.5/11.1	2.16/1.33	17/10	>20	1	0.24 × 0.25	>15	2.11	3.55	0.5	0.0027
[87]	3.4/5.2	5.8/11.8	1.2/1.4	23/32	>30	2	0.25 × 0.12	>15	2.35	3.55	0.8128	0.0022
[61]	1.575/2.4	6/3.8	0.9/1.1	30/20	>50	1	0.5 × 0.35	>38	3.37	2.2	0.787	0.0009
[88]	1.0/1.5	4/3.3	1.58/1.54	16/15	>38	1	0.28 × 0.34	>30	3.3	4.4	0.8	0.018
[89]	2.4/5.2	8.3/4.8	0.53/0.59	10/13	>60	1	0.4 × 0.103	>15.5	5.42	2.22	0.381	0.0009
[90]	2.45/5.25	7/5	1.96/2.25	14/16	>25	2	0.07 × 0.09	>25	4.08	3.66	0.508	0.004

Accordingly, researchers have studied the stub-loaded dual-mode resonators as an alternative structure as reviewed in the next section.

4.3 *Stub-loaded dual-mode resonators (SLDMR)*

The stub-loaded dual-mode resonators (SLDMRs) are essentially resonators that support two resonant modes. They consist of a main transmission line coupled with stubs (short-circuited or open-circuited) at specific locations along the main line. These stubs introduce additional resonant modes, allowing for the creation of dual-band responses. SLDMRs enable the integration of multiple resonant modes in a compact structure ($0.14\lambda_g \times 0.11\lambda_g$), resulting in a smaller filter size. They offer a simpler and more efficient design process compared to traditional approaches. Moreover, the resonant frequencies can be adjusted by varying the dimensions of the stubs and transmission line, providing flexibility in meeting different system requirements. Accordingly, they can exhibit higher selectivity (510 dB/GHz) and improved out-of-band rejection (more than 35 dB) compared to single-band filters. In this context, different SLDMR-based compact filters have been proposed in [91–101]. For instance, the filter proposed in [91] employs a stepped-impedance ring resonator loaded with shorted stubs, achieving a remarkably wide upper stopband ($>$ 40 dB up to $4.85f_{01}$) and excellent in-band performance (IL $<$ 0.28 dB, RL $>$ 25 dB, isolation $>$ 50 dB). However, the filter size is relatively large ($0.50\lambda_g \times 0.39\lambda_g$) due to the ring resonator structure. Meanwhile, the filter of [92] uses stub-loaded Open-Loop Resonators (OLRs) with a focus on narrowband dual-band operation (2% and 3% FBW at 2.45 and 5.8 GHz). The compact size ($0.4\lambda_g \times 0.4\lambda_g$) and

moderate upper stopband rejection (> 20 dB up to $4.08f_{01}$) are its key attributes. The narrow fractional bandwidth is a deliberate design choice suited to applications requiring high channel selectivity. Later, the work has been extended in [94], where a compact dual-wideband bandpass filter (FBW: 9.42% and 7.76% at 3.5/5.5 GHz) using open-/short-circuited stubs has been proposed. The moderate size ($0.32\lambda_g \times 0.15\lambda_g$), low insertion loss (0.7/1.1 dB), and good stopband rejection (> 35 dB up to $2.29f_{01}$) make it suitable for WLAN/5G sub-6 GHz applications.

Accordingly, some new types of stub-loaded coupled-line and ring resonator structures have been proposed in [95–104]. For instance, in [95], E-type hairpin resonators have been employed, which are basically the short-circuited stub-loaded hairpin resonators. The passband frequencies have been controlled by adjusting the characteristic impedance and electrical length of the hairpin and stub (Figure 6). Moreover, by incorporating a pseudo-interdigital coupling structure and a hook feed line in the structure passband bandwidth has been greatly controlled. The designed filter provides exceptional compactness ($0.14\lambda_g \times 0.11\lambda_g$) with good stopband suppression (> 35 dB up to $3.27f_{01}$). The controllable bandwidth feature via the pseudo-interdigital coupling structure is a key novelty. In this context, filter proposed in [96] achieves very wide dual-band FBW (43.2%/16.5%) using folded short-circuited stubs with low insertion loss (0.33/0.74 dB), though the upper stopband is limited (> 12 dB). In [97], open-/short-circuited stub-loaded $\lambda/4$ resonators have been employed for a compact filter design with moderate stopband rejection (> 20 dB up to $3.75f_{01}$). Meanwhile, ref. [98] demonstrates filter design with broadly-separated passbands (1.8/5.8 GHz) and sharp rejection level (> 30 dB) using balanced coupled lines loaded with folded open-circuited stubs. However, a wide-band filter is proposed in [99] with FBW (51.9%/23.3%) using dual-mode folded resonators. The upper stopband rejection level has been achieved as better than 30 dB up to $3.33f_{01}$. Afterwards, a high selectivity dual-band filter has been proposed in [100], where a quadruple-mode multi-stub loaded ring resonator was employed to achieve a size of $0.44\lambda_g \times 0.30\lambda_g$. In this context, the filter of [101] combines stub-loaded hairpin resonators with meandering UIRs for a balanced performance compromise.

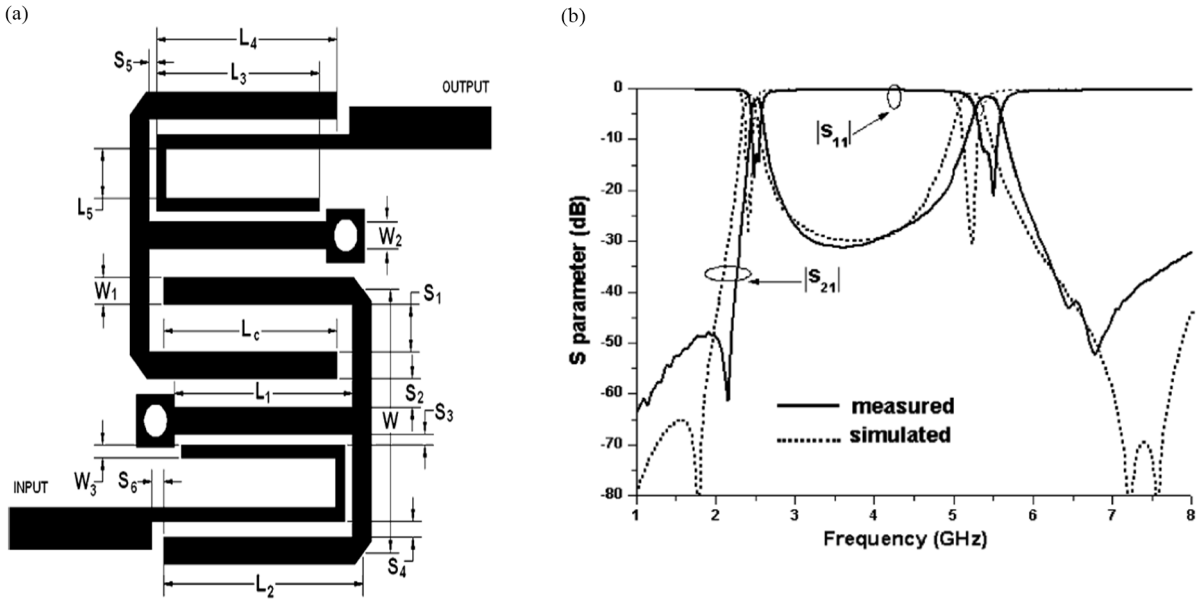

Figure 6. (a) Layout of the proposed filter with dimensions labeled; (b) frequency responses of the simulated and measured results [95]

For all such filters [95–101], the main investigation has been concentrated on the enhancement of skirt selectivity (475 dB/GHz), the achievement of good isolation between the passbands with a reasonable rejection level (more than 30 dB), the generation of multiple transmission zeros (more than 7), the improvement of in-band performance like reduction of insertion loss (0.2 dB) and increase of return loss (more than 25 dB), and the attainment of a compact filter size ($0.28\lambda_g \times 0.2\lambda_g$). However, for those filters, the performance beyond the second passband is limited to $3f_0$ with a rejection level limited to 25 dB. Accordingly, the enhanced upper out-of-band rejection has been studied in [102–104] by employing different

methodologies based on stub-loaded resonators. In [102], a wide upper stopband rejection bandwidth up to $5.7f_{01}$ with a rejection level of 30 dB has been achieved by simply tuning the length and impedance of the symmetrical open-circuited stub-loaded resonators. Subsequently, dual-band filters with closely spaced narrow passbands (3.81 GHz/4.2 GHz) and improved stopband rejection have been proposed by coupling shorted lines in a stub-loaded resonator in [103] (more than 20 dB up to $2f_{01}$), and by a loop-type microstrip line loaded with four shorted stubs in [104]. However, the size of the filter in [104] is quite large ($0.39\lambda_g \times 0.46\lambda_g$) compared to those in [102] ($0.47\lambda_g \times 0.33\lambda_g$) and [103] ($0.32\lambda_g \times 0.28\lambda_g$). Table 7 highlights the comparative study of some of the best filters reported by dual-mode resonators loaded with stubs. It has been observed that the filter in [95] (shaded by gray color) has provided the best performance.

To sum up, although stub-loaded dual-mode resonators (SLDMRs) have several benefits, they do, however, have several drawbacks, such as limited bandwidth (2%–30%) due to fixed resonant frequencies, complex design process requiring precise control of dimensions, sensitivity to fabrication tolerances leading to performance variations, limited scalability to higher frequencies or different applications, challenges in achieving adequate coupling and isolation between resonators, limited reconfigurability or tunability once fabricated. SLDMRs are nonetheless useful for designing compact multi-band filters in spite of these disadvantages; thus, considerable thought must be given to them both during the design and optimization phases.

Table 7. Comparative study of dual-band bandpass filters based on stub-loaded dual-mode resonators

Ref. no.	f_{o1}/f_{o2} (GHz)	3-dB *FBW* (%)	*IL* (dB)	*RL* (dB)	*MSRL* (dB)	*TZs*	Size $\lambda_g \times \lambda_g$	*USBRL* (dB)	*USBW* ($\times f_{o1}$)	Substrate specifications		
										ε_r	h (mm)	$\tan\delta$
[91]	1.84/2.9	8.1/6.8	1.7/1.6	20/20	>55	1	0.50 × 0.39	>30	2.44	6.15	0.635	0.0019
[92]	2.45/5.8	2/3	1.87/1.68	20/15	>20	2	0.4 × 0.4	>20	4.08	2.2	0.381	0.0009
[94]	3.5/5.5	9.42/7.76	0.7/1.1	21/14	>30	1	0.32 × 0.15	>35	2.29	3.38	0.813	0.0027
[95]	2.45/5.25	6.8/5.1	1.7/1.5	15/20	>25	1	0.14 × 0.11	>35	3.27	9.5	0.635	0.0004
[96]	2.48/6.63	43.2/16.5	0.33/0.74	18/30	>20	1	0.12 × 0.17	>12	4.23	2.2	0.508	0.0009
[97]	2.4/5.8	4.36/3.6	1.35/1.97	17/15	>25	2	0.39 × 0.25	>20	3.75	2.55	0.8	0.0029
[98]	1.8/5.8	8.9/4.5	1.2/2.0	24/25	>30	2	0.37 × 0.28	>30	4.72	2.55	0.8	0.0029
[99]	2.4/5.2	51.9/23.3	0.3/07	22/21	>25	2	0.28 × 0.20	>30	3.33	2.55	0.8	0.0029
[100]	2.4/5.2	10.5/5.5	1.37/1.23	32/19	>14	2	0.30 × 0.33	>17	5.3	10.8	1.27	0.002
[101]	2.65/4.84	6.04/8.7	0.99/1.39	16/15	>19	2	0.44 × 0.30	>30	2.45	11.2	1.27	0.001
[102]	3.5/5.25	6.5/4.3	1.87/2.33	22/21	>40	2	0.47 × 0.33	>28	5.7	2.55	0.8	0.0029
[103]	3.81/4.2	3.2/5.7	1.05/0.85	24/19	>26	1	0.32 × 0.28	>20	2.36	3.38	0.508	0.0027
[104]	1.84/2.45	1.5/2.2	1.6/1.3	20/22	>30	2	0.39 × 0.46	>20	1.43	2.55	0.8	0.0029

4.4 *Dual-mode filter with combination of SIRs and stubs*

A dual-mode dual-band bandpass filter based on Stepped-Impedance Stub-Loaded Resonators (SISLR) offers a compact and efficient solution for filtering signals in two distinct frequency bands simultaneously, making it suitable for various wireless communication and RF and microwave applications. With the attractive resonating features of both stepped-impedance resonators and stubs, researchers have utilized both of them together in a single filter structure for

their efficient performances. In this context, asymmetric stepped-impedance open-loop resonators loaded with stubs have been employed in [105] to improve the selectivity of the passbands (540 dB/GHz). However, the passbands are widely separated from each other in [105] (0.9 GHz/2.45 GHz). Later, dual-mode stepped-impedance stub resonators [83] and stub-loaded stepped-impedance resonators [106] have been employed to design compact dual-band filters. However, the size of the filter in [106] ($0.47\lambda_g \times 0.47\lambda_g$) has quite a large area compared to that of [83] ($0.17\lambda_g \times 0.21\lambda_g$). However, for all such filters, the upper out-of-band performance has been unexplored. Subsequently, a combination of coupled lines and tri-stepped impedance stubs [107], a multi-stub loaded resonator [109], a stepped-impedance ring resonator with shorted stubs [91] (Figure 7), and a combination of pairs of step impedance stubs, and a pair of uniform open-circuit stubs [109] are the novel structures investigated. In [91], a wide upper stopband (more than 40 dB up to $4.85f_{01}$) along with overall improved passbands' performance (insertion loss less than 0.28 dB, return loss more than 25 dB and isolation level between the passbands more 50 dB) has been achieved. However, the sizes of the filters in [108] ($0.93\lambda_g \times 0.26\lambda_g$) and [91] ($0.5\lambda_g \times 0.39\lambda_g$) are quite large compared to [109] ($0.13\lambda_g \times 0.1\lambda_g$). Table 8 highlights the comparative study of the dual-mode dual-band bandpass filters loaded with stepped-impedance stubs. It has been revealed that the filter in [91] has contributed the best performances.

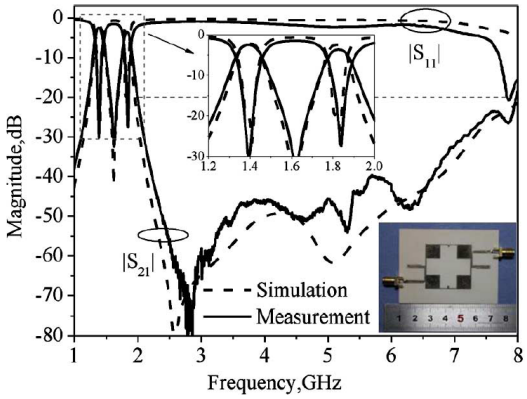

Figure 7. Photograph of the fabricated filter with dimensions labeled (inset figure) and frequency responses of the simulated and measured results [91]

Table 8. Comparative study of dual-band bandpass filters based on stub-loaded dual-mode resonators with SIRs

Ref. no.	f_{o1}/f_{o2} (GHz)	3-dB *FBW* (%)	*IL* (dB)	*RL* (dB)	*MSRL* (dB)	*TZs*	Size $\lambda_g \times \lambda_g$	*USBRL* (dB)	*USBW* ($\times f_{o1}$)	Substrate specifications		
										ε_r	*h* (mm)	$\tan\delta$
[105]	0.9/2.45	6/4.8	1.1/1.0	15/22	>20	3	0.20 × 0.13	>20	3.89	2.94	0.762	0.0025
[83]	1.84/2.65	20/10	0.43/0.65	14/16	>25	1	0.17 × 0.21	>25	2.17	2.65	1.0	0.001
[106]	2.45/5.85	5.7/4.6	1.5/2.4	12/13	>30	1	0.47 × 0.47	>20	3.3	3.38	0.813	0.0027
[107]	0.92/1.52	38/22.4	1.01/0.96	14/16	>30	1	0.13 × 0.41	>15	3.26	2.33	1.6	0.0012
[108]	2.4/3.5	8.3/5.14	2.8/4.5	15/13	>50	2	0.93 × 0.26	>50	2.29	2.55	0.8	0.0029
[91]	1.4/1.83	9.3/6.6	2.48/3.6	28/25	>28	1	0.50 × 0.39	>40	4.85	3.38	0.813	0.0027
[109]	0.94/2.48	39/27	0.28/0.92	25/12	>30	2	0.13 × 0.10	>25	5	4.4	0.8	0.02

The advantages of this category of filters are listed as follows:

• **Ultra-compact filter sizes:** The combination of SIRs and stub-loading enables very compact designs. The filter proposed in [109] achieves the smallest size in this category ($0.13\lambda_g \times 0.10\lambda_g$), and those in [105] ($0.20\lambda_g \times 0.13\lambda_g$) and in [83] ($0.17\lambda_g \times 0.21\lambda_g$) are also highly compact, demonstrating the superior miniaturization capability of this topology compared to the PCR-based designs reviewed in Section 3.1.

• **Very Low Insertion Loss:** The filter proposed in [109] achieves the lowest insertion loss in this category (0.28/0.92 dB at 0.94/2.48 GHz), and that in [83] also reports competitive insertion loss (0.43/0.65 dB). This is attributed to the reduced conductor length achievable with SIR stub-loading.

• **Wide Fractional Bandwidth Capability:** Unlike some other topologies reviewed, SISLR-based filters can accommodate very wide fractional bandwidths. For example, the filter designed in [109] achieves 39%/27% of FBW, and [107] achieves 38%/22.4% of FBW, enabling their use in wideband communication standards.

• **Excellent Middle Stopband Rejection Level (MSRL):** The filter proposed in [91] achieves MSRL of > 40 dB and that in [108] achieves MSRL of > 50 dB, indicating very high isolation between the two passbands. It is a critical requirement for multi-standard transceivers to prevent inter-band interference.

• **Wide Upper Stopband:** The filter designed in [91] achieves a wide upper stopband of > 40 dB up to $4.85f_{01}$, and that in [109] achieves upper stopband of > 25 dB up to $5f_{01}$, both of which are competitive figures in the context of all design categories reviewed.

The limitations of this category of filters are listed as follows:

• **Higher Insertion Loss for Some Designs:** The filter of [108] reports significant insertion losses (2.8/4.5 dB) and that of [91] reports (2.48/3.6 dB), considerably higher than the best values in the PCR-SIR or metamaterial categories. This is attributed to the combined losses of the SIR and stub elements in larger filter structures.

• **Large Physical Size for Some Entries:** Despite the category's potential for compactness, the filters designed in [91] (size: $0.50\lambda_g \times 0.39\lambda_g$) and [108] (size: $0.93\lambda_g \times 0.26\lambda_g$) are considerably large in size, indicating that incorporating SIR ring resonators with stub-loading does not always guarantee miniaturization.

• **Limited Return Loss for Some Designs:** The filter proposed in [106] reports return losses (RL) of only 12/13 dB, and that in [105] reports 15/22 dB, indicating incomplete impedance matching and that passband quality may be insufficient for stringent communication standards requiring RL > 20 dB.

• **Fixed Resonant Frequencies (No Tunability):** All designs in Table 8 are fixed-frequency, with resonant frequencies entirely determined by physical dimensions. This contrasts with the metamaterial-based tunable filters reviewed in Section 7 and represents a fundamental limitation for reconfigurable or cognitive radio applications.

Other than these limitations as observed from Table 8, dual-mode dual-band bandpass filters loaded with SISLRs have some more limitations, such as complex design process and fabrication complexity requiring precise control over resonator and stub dimensions, limited bandwidth tunability due to fixed resonant frequencies determined by physical dimensions, sensitivity to parasitic effects, limited scalability, difficulty in achieving adequate coupling and isolation between resonators and challenges in scaling filters to different frequencies or applications. Despite these limitations, SISLR-based DMDBBPFs remain valuable for applications requiring simultaneous filtering of signals at two distinct frequency bands, with careful consideration during design and optimization.

5. Fractal based dual-band filters

Fractal curves provide the possibility of creating infinite-length lines on a finite substrate area. Fractals offer several advantages in filter design, such as compactness due to the space-filling property, multi-band capability and consistent performance across a wide range of frequencies due to the self-similarity property, flexibility in design parameters in terms of bandwidth, center frequency, and stopband attenuation with greater precision, wideband performance, and ease of fabrication and integration into various electronic devices and systems [110]. In this context, different fractal geometries have been employed by the researchers in the design of compact high-selectivity dual-band bandpass filters, such as the Koch fractal in [111] and the Minkowski fractal in [112–114]. For instance, Minkowski-Island-Based (MIB) fractal patch

resonators have been proposed in [112] to design a compact dual-band filter with enhanced performance as shown in Figure 8a. Koch fractals offer several advantages for dual-band filter design, including compact size ($0.23\lambda_g \times 0.23\lambda_g$), tunability of passband bandwidths (4.6%–15%), low losses (less than 0.25 dB), and enhanced frequency selectivity (470 dB/GHz) as explored in Figure 8b. However, their design complexity, limited design flexibility, non-conventional structure, sensitivity to manufacturing imperfections, and limited bandwidth coverage are notable challenges. Meanwhile, Minkowski fractals provide special benefits such as flexibility in controlling the fractal dimensions, compactness ($0.19\lambda_g \times 0.19\lambda_g$), and adaptability for processing diverse types of signals.

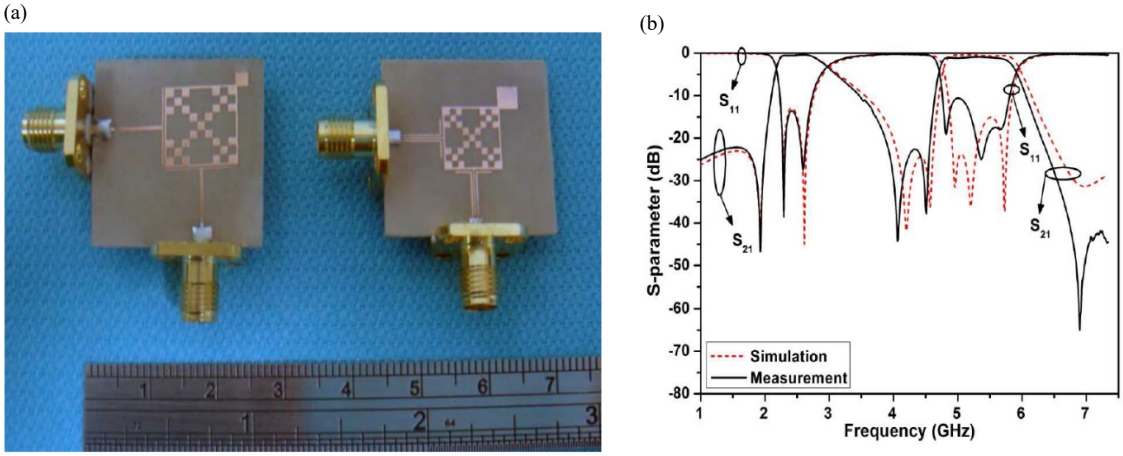

Figure 8. (a) Photograph of the fabricated filter with dimensions labeled; (b) Frequency responses of the simulated and measured results [112]

Despite many advantages, it also suffers from increased design complexity, the requirement of intensive computation for fractal dimensions, and limited analytical understanding due to the finite boundary, especially when dealing with signals or images with non-periodic characteristics. As an alternative, square-shaped Sierpinski fractal geometry has been utilized in [115, 116] and triangular-shaped Sierpinski fractal geometry has been employed in [117]. As a result, dual-band filters with the advantages of compactness ($0.31\lambda_g \times 0.35\lambda_g$), fine-tuning of characteristics, and reduced cross-coupling between the two frequency bands, enhanced selectivity (492 dB/GHz), and rejection of unwanted frequencies have been obtained (rejection level more than 33 dB up to $3.26f_{01}$). However, like Minkowski fractals, Sierpinski fractal-based filters are also suffering from complex design processes, manufacturing challenges, limited bandwidth (3.3%–45%), and sensitivity to environmental factors such as temperature variations or substrate properties. Later, different types of fractal geometries have also been investigated for dual-band filters, such as the T-square fractal [118] and the Hilbert fractal resonator [119] to achieve more compactness ($0.22\lambda_g \times 0.21\lambda_g$) and a rejection level more than 20 dB up to $2.04f_{01}$. Table 9 highlights the comparative study of the fractal-based dual-band bandpass filters. It has been observed that the filter in [112] (shaded by gray color) has contributed the best performances. All such filters have the advantages of compactness ($0.19\lambda_g \times 0.19\lambda_g$) and high selectivity (more than 450 dB/GHz). However, such filters are also suffering from some limitations in terms of limited bandwidth due to the inherent nature of fractal geometries, complex design and optimization processes to achieve dual-band operation, sensitivity to fabrication tolerances, leading to performance variations, challenges in scaling filters to different frequencies or applications, manufacturing complexities and cost considerations, and cross-coupling between passbands, affecting filter performance.

In summary, it can be concluded that fractal geometries are quite effective in designing dual-band filters with compact size, customizable characteristics, and reduced cross-coupling between frequency bands, making them attractive for certain applications in communications. As an alternative approach, defected ground structures have been studied by the researchers for the designing of dual-band filters as explored in the next section.

Table 9. Comparative study of dual-band bandpass filters based on fractals

Ref. no.	f_{o1}/f_{o2} (GHz)	3-dB FBW (%)	IL (dB)	RL (dB)	$MSRL$ (dB)	TZs	Size $\lambda_g \times \lambda_g$	$USBRL$ (dB)	$USBW$ ($\times f_{o1}$)	Substrate specifications		
										ε_r	h (mm)	$\tan\delta$
[111]	0.82/2.17	15/4.6	0.75/1.85	25/20	>22	1	0.23 × 0.23	>26	4.27	10.2	0.635	0.0023
[112]	2.55/5.27	29.8/21	0.35/0.86	15/10	>23	2	0.19 × 0.19	>42	2.94	10.2	1.27	0.0023
[114]	2.41/3.29	7.3/4.4	0.56/0.62	35/	>50	1	0.21 × 0.25	>10	1.74	10.8	1.27	0.002
[115]	4.3/8.6	45/14	0.6/1.8	12/15	>38	2	0.31 × 0.35	>33	3.26	3.38	0.508	0.0022
[116]	2.39/3.45	5.7/3.3	0.9/0.49	23/20	>40	1	0.49 × 0.49	>20	1.88	10.8	1.27	0.002
[119]	2.45/3.5	8.7/3.18	0.38/2.53	19/10	>27	2	0.22 × 0.21	>20	2.04	2.2	1.575	0.0009

6. Defected ground structure based dual-band filters

Defected ground structures (DGS) are the most basic multi-layer structures realized in printed circuit board technology, with two categories. DGS structures have some advantages, like enabling compact filter designs with high selectivity, allowing simultaneous filtering at two distinct frequency bands within a single device, being well-suited for integration into various RF and microwave circuits and systems, and achieving relatively low insertion loss. DGS structures with resonators realized in both the ground layer and the conductive layer make up the first group. However, DGS filters, whose resonators have only been realized in the ground layer, are included in the second category. Since resonators realized in two layers are coupled over the whole area and not just through the edges, the first type of filter aims to reduce circuit size while increasing coupling between the resonators. The first category of DGS structures has been employed in [120, 121]. A second category has been employed in [122]. However, both types of filters typically don't show both good passband performance (isolation is limited to only 25 dB) and compactness ($0.38\lambda_g \times 0.34\lambda_g$) at the same time. Later, somewhat more complicated structures with two distinct conductive layers positioned above the ground layer are proposed in [123]. Accordingly, passbands isolation level more than 20 dB and compactness of $0.32\lambda_g \times 0.32\lambda_g$ has been achieved.

Subsequently, many researchers have employed different types of DGS structures to design compact dual-band filters with improved performance. In this context, tunability of the second passband has been achieved in [124] by employing a stub-loaded resonator (SLR) with the help of a defected ground structure (DGS) transmission line and varactor diodes. Later, composite right/left handed (CRLH) triangle mushroom structure and defected ground structure (DGS) were combined in [125] to achieve low in-band insertion loss (1.13 dB), compact size (550 mm^2), and enhanced out-band rejection (more than 30 dB up to $3.26f_{01}$) for the dual-band filter. Henceforth, in [126], by introducing a pair of coupling stubs in the aperture of the DGS, narrow passbands (4% and 3.1%) has been achieved within a wide stopband (9.65 GHz to 12 GHz). Subsequently, a single meander multimode DGS resonator in [127], a combination of SIR and DGS in [128], a combination of a varactor- and stub-loaded Dumbbell-shaped resonator (VSDSR) with DGS in [129], stepped-impedance DGS and embedded folded slot line on the ground structure [130], and hybrid microstrip/DGS dual-resonance cells in [131] have been proposed. For instance, in [131] two filters have been proposed based on stepped-impedance DGS and embedded folded slotline on the ground (Figure 9). Both the dual-band BPFs exhibit the ultra-wide upper stopband, extended up to 40 GHz ($11.54f_{01}$) with a high rejection level about 30 dB (Figure 10). Table 10 highlights the comparative study of the DGS-based dual-band bandpass filters. It has been observed that the filter in [131] has exhibited the best performances. However, they face limitations stemming from design complexity, as optimizing for dual-band operation can be intricate. Additionally, achieving desired performance metrics at both bands often involves trade-offs, and the filters are sensitive to fabrication variations, necessitating tight tolerances.

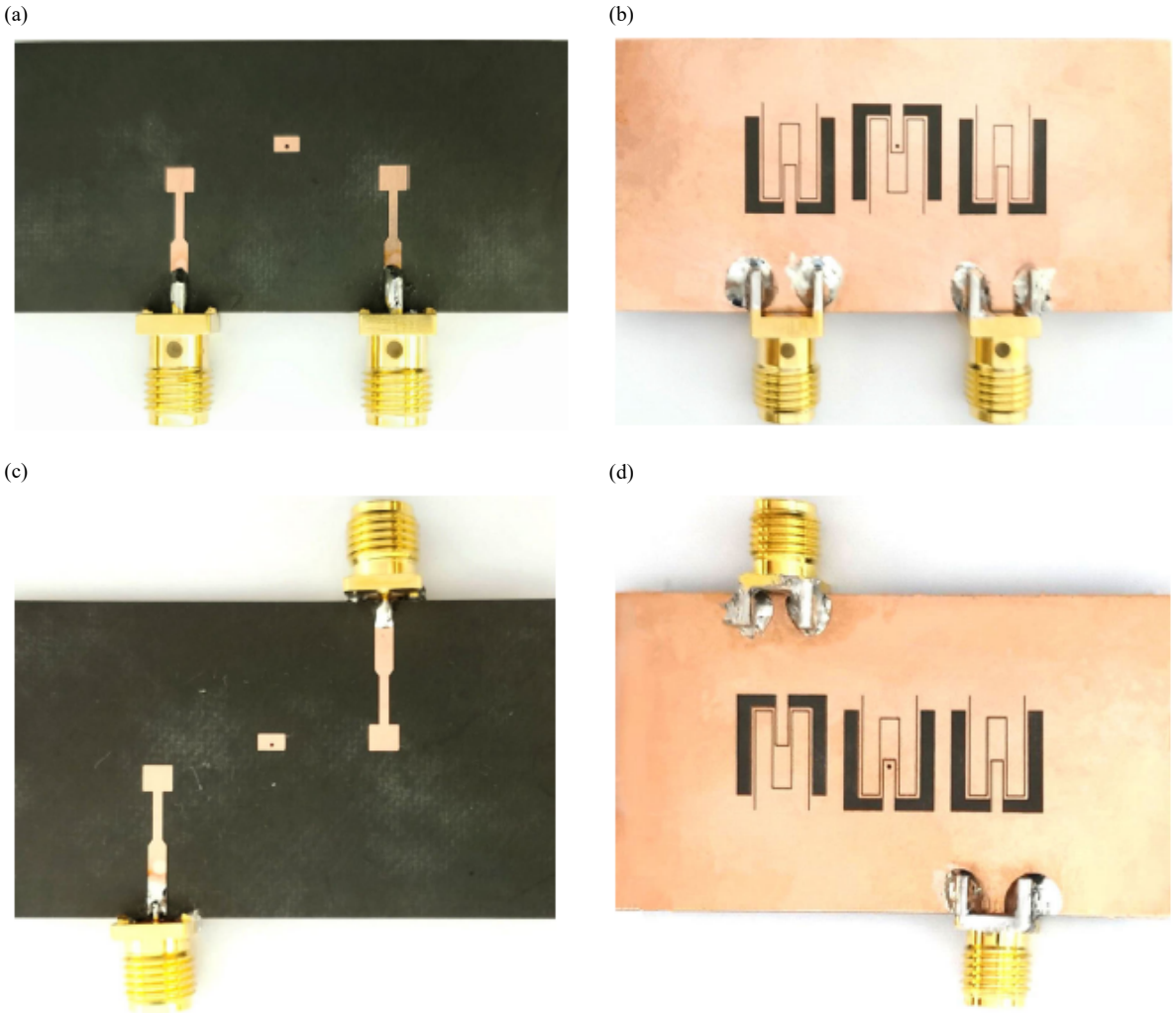

Figure 9. Photograph of the developed dual-band BPF prototypes, (a) Top view and (b) bottom view of Type-I BPF; (c) Top view and (d) bottom view of Type-II BPF [131]

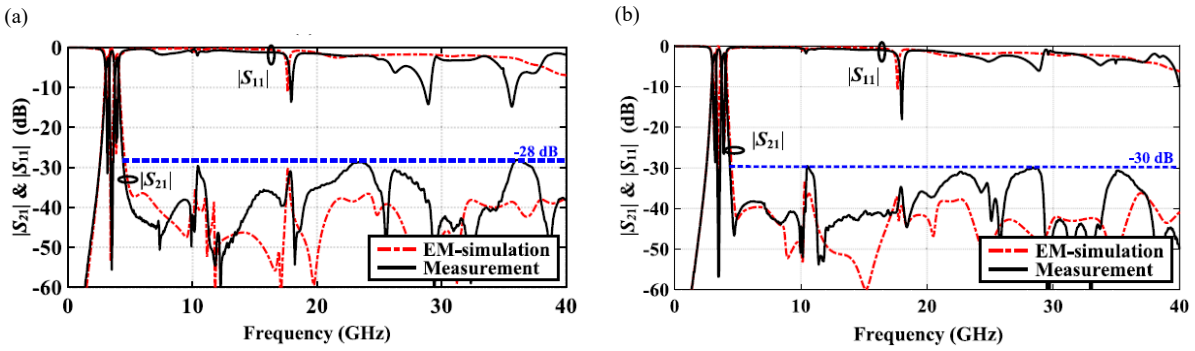

Figure 10. (a) Wideband response of BPF-I; (b) Wideband response of BPF-II [131]

Table 10. Comparative study of dual-band bandpass filters based on defected ground structures (DGSs)

Ref. no.	f_{o1}/f_{o2} (GHz)	3-dB *FBW* (%)	*IL* (dB)	*RL* (dB)	*MSRL* (dB)	*TZs*	Size $\lambda_g \times \lambda_g$	*USBRL* (dB)	*USBW* ($\times f_{o1}$)	Substrate specifications		
										ε_r	*h* (mm)	$\tan\delta$
[120]	2.35/3.15	4/3	1.8/3.0	20/28	>45	1	0.23 × 0.14	>23	1.91	2.65	1.0	0.001
[121]	2.4/5.2	20/10	0.4/0/58	20/20	>17	3	0.38 × 0.34	>20	3.96	2.2	0.787	0.0009
[122]	1.85/2.35	5.5/4.5	0.5/1.0	15/15	>30	1	0.18 × 0.24	>15	2.16	2.65	1.0	0.001
[123]	2.44/3.28	8.1/4.2	1.2/1.5	20/20	>45	1	0.21 × 0.17	>30	3.69	3.38	0.508	0.0027
[124]	1.7/2.15	8/7	3.5/4.8	15/15	>20	2	0.32 × 0.32	>25	1.76	9.6	0.8	0.002
[125]	1.58/2.56	16.8/7.5	0.59/1.44	15/14	>30	1	0.31 × 0.22	>25	3.8	2.2	0.787	0.0009
[126]	3.68/8.8	52/3.4	1.37/1.13	15/16	>20	1	0.26 × 0.24	>30	3.26	2.2	0.508	0.0009
[127]	2.58/5.86	12.8/14.7	1.1/1.0	15/17	>22	2	0.09 × 0.08	>10	3.1	2.65	1.0	0.001
[129]	2.4/3.5	5.8/7.7	2.0/2.2	25/22	>35	2	0.32 × 0.22	>20	2.29	3.5	0.508	0.0018
[131]	3.12/3.87	9.6/7.5	4.35/4.52	21/14	>22	1	0.42 × 0.56	>28	11.54	2.2	0.508	0.0009

Their limited frequency agility may restrict adaptability to wideband applications, and the close proximity of bands may result in crosstalk and unwanted coupling effects, affecting filter performance and isolation between bands.

7. Metamaterial based tunable dual-band filters-recent advances

Recently, metamaterial structures have been investigated by the researchers to achieve tunablity feature in dual-band filters. Artificial materials designed to possess characteristics not present in naturally occurring materials are called metamaterial. In order to control electromagnetic waves in novel ways, they are made up of sub-wavelength structures that are frequently stacked in periodic arrays. Metamaterial structures have the advantages such as: (1) they resonate at specific frequencies suitable for the design of bandpass filter; (2) they can enable the bandpass filter to achieve higher bandwidth (more than 40%) and sharper selectivity (better than 500 dB/GHz); (3) they can exhibit switchable properties, allowing the bandpass filter to dynamically switch between different frequency bands; and (4) they can achieve compact and light weight designs, which is advantageous for integrating the bandpass filter into portable devices. Tunable dual-band bandpass filters made of metamaterials are a fascinating area of research and development in the fields of microwave and RF engineering. One approach for achieving tunable dual-band bandpass filters is by incorporating varactor diodes [132–137] and some or other tunable elements into the metamaterial structure [138–140]. Varactor diodes are semiconductor devices whose capacitance can be controlled by applying a voltage across them. By integrating varactors into the metamaterial structure, the effective properties of the metamaterial can be dynamically modified, allowing for tunable filtering characteristics. For instance, in [138], defected ground structures have been employed at input and output feeding lines to suppress the harmonics to a rejection level more than 20 dB up to $10f_{01}$ (Figure 11). Another approach involves using reconfigurable metamaterial structures, where the geometry or configuration of the metamaterial elements can be altered to change the filtering behavior. This can be achieved using techniques such as liquid crystal-based tuning mechanisms [139] and MEMS (Micro-Electro-Mechanical Systems) [140]. Table 11 highlights the comparative study of the metamaterial-based dual-band bandpass filters. It has been revealed that a wide upper stopband bandwidth up to $10f_0$ with a rejection level

of more than 20 dB has been achieved as an optimum result for the filter proposed in [138]. Moreover, the attenuation level better than 30 dB between the passbands has been reported. The size of the filter is quite compact ($0.18\lambda_g \times 0.19\lambda_g$). Metamaterial-based tunable dual-band bandpass filters provide unique capabilities but face many limitations.

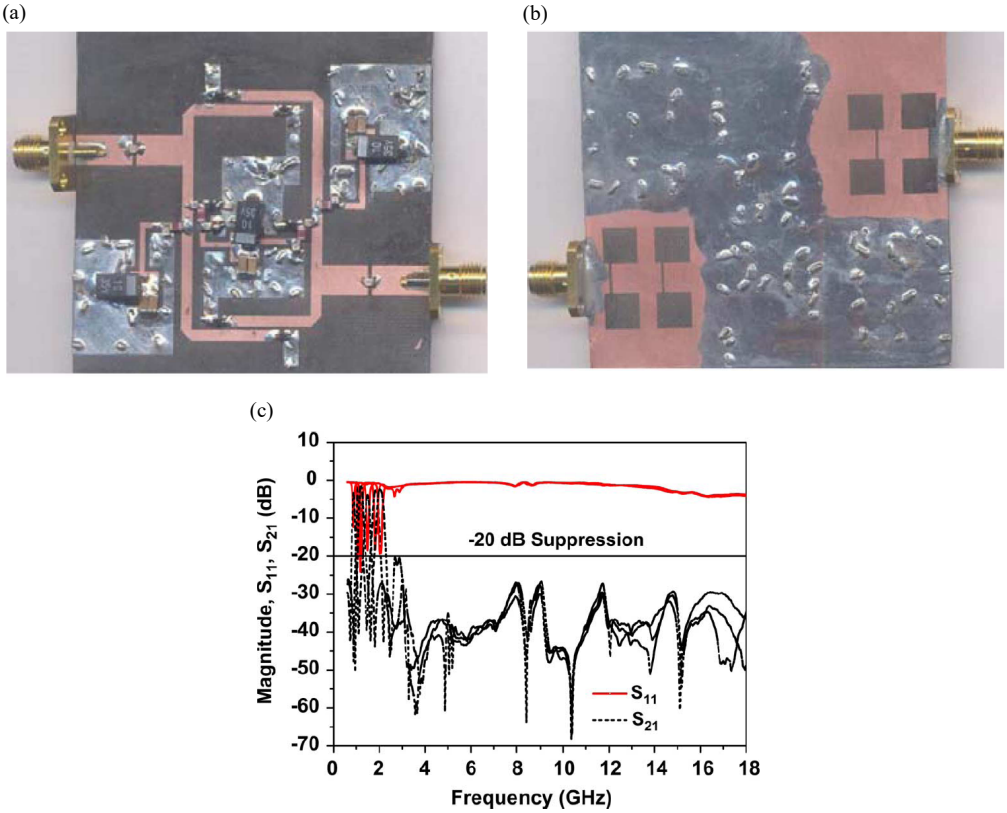

Figure 11. Photograph of fabricated filter II, (a) Top side; (b) Bottom side; (c) measured broadband harmonic suppression characteristics of filter II in overall tuning range passbands [138]

Some of the limitations are such as requirement of costly and complex fabrication process, introduction of metallic and dielectric losses, limited tuning range and tuning speed of the filter, nonlinear behavior and lower power handling capacity, sensitivity to temperature variations, complexity for the integration into existing systems, and high production costs and scalability issues. Moreover, the harmonics suppression level is limited to 20–25 dB, restricting applications in mixers and frequency synthesizers. Ongoing research aims to overcome these limitations to fully harness the potential of metamaterials in tunable filter design. Finally, Table 12 compares the performances of all the best designs for each category of filter design discussed so far. It has been observed that Cross-Coupled Resonator (CCR) based and Dual-Mode Stub-Loaded Stepped-Impedance Resonator (DM-SLSIR) based dual-band filters have exhibited compact sizes, more than 40 dB of upper stopband rejection level and extension of the upper stopband bandwidth greater than $4.2f_{01}$. The DGS based filter exhibits higher insertion loss and poor isolation level between the passbands. Moreover, design complexity is more for DGS based filter as both sides of the substrate are required to be perturbed. Out of all methods, only the metamaterial-based filter provides the tunability facility of the passbands along with a very wide upper stopband rejection bandwidth upto $10f_{01}$, with a restriction of rejection level of only 20 dB. In summary, it is to be concluded that all the methods have some advantages and some limitations. There are many research issues are still left to study in detail for the designing of microstrip-line based dual-band pass filters to fulfill the demands in modern days wireless communication systems.

Table 11. Comparative study of metamaterial based tunable dual-band bandpass filters

Ref. no.	Tunable Freq. (GHz)		3-dB FBW variation (%)		IL (dB)		RL (dB)		Size $\lambda_g \times \lambda_g$	MSBRL/ USBRL (dB)	USBW $\times f_{o1}$	Substrate specifications		
	f_{o1}	f_{o2}	f_{o1}	f_{o2}	f_{o1}	f_{o2}	f_{o1}	f_{o2}				ε_r	h (mm)	$\tan\delta$
[132]	2.45 (fixed)	5.25–5.75	8.6	6.7	1.8	2.3–4.5	13	>10	0.22 × 0.12	>55/20	2.85	3.55	0.813	0.0027
[133]	0.77–1.02	1.57–2.0	20.3–24.7	8.15-5.6	0.7–1.4	2.74–3.93	>12	>15	0.14 × 0.1	>50/20	3.63	2.65	0.8	0.0002
[134]	0.88-1.12	1.5–1.81	5.4–6.4	5.1–6.4	1.65–4.3	3.11–3.9	13	>10	0.18 × 0.19	>35/30	2.61	3.5	0.762	0.004
[135]	0.81–0.95	1.51–1.79	4.2–5.0	6.8–8.0	2.1–3.3	2.37–3.26	>10	>10	0.25 × 0.22	>25/22	2.72	3.5	0.762	0.004
[137]	2.2–2.7	3.45–4.2	22.2	19.6	<4	<4.5	NR	NR	0.68 × 0.55	>20/20	3.18	3.48	0.51	0.001
[138]	0.85–1.2	1.4–2.14	13	11	1.31–3.4	1.8–3.8	>13	>13	0.15 × 0.22	>30/20	10	2.2	0.787	0.0009
[139]	1.48–1.80	2.4–2.88	5.7–8.5	8.2–12.4	1.99–4.4	1.6–4.2	>12	>13	0.35 × 0.24	>24/20	10	2.2	0.787	0.0009

Table 12. Comparative study of dual-band bandpass filters

Ref. no.	f_{o1}/f_{o2} (GHz)	Method	3-dB *FBW* (%)	*IL* (dB)	*RL* (dB)	*MSRL* (dB)	Size $\lambda_g \times \lambda_g$	*USBRL* (dB)	*USBW* ($\times f_{o1}$)
[22]	0.58/1.31	FTM	39.6/18.3	0.3/0.9	21/23	>50	0.04 × 0.54	>30	3.45
[41]	2.4/5.2	PC-SIR	6/4	2.49/2.79	16/17	>60	0.18 × 0.16	>30	8.3
[65]	1.57/2.7	CCR	3.17/2.09	0.54/0.8	22/25	>58	0.39 × 0.26	>40	4.27
[67]	2.4/5.8	DMR-P	12/12	1.4/3.2	20/28	>10	0.33 × 0.15	>50	2.92
[61]	1.575/2.4	DM-SIR	6/3.8	0.9/1.1	30/20	>50	0.5 × 0.35	>38	3.37
[95]	2.45/5.25	DMR-SL	6.8/5.1	1.7/1.5	15/20	>25	0.14 × 0.11	>35	3.27
[91]	1.4/1.83	DM-SISLR	9.3/6.6	2.48/3.6	28/25	>28	0.50 × 0.39	>40	4.85
[112]	2.55/5.27	FRACTAL	29.8/21	0.35/0.86	15/10	>23	0.19 × 0.19	>42	2.94
[130]	3.12/3.87	DGS	9.6/7.5	4.35/4.52	21/14	>22	0.42 × 0.56	>28	11.54
[138]	0.85-1.2/ 1.4–2.14	META-MATERIAL	13/11	1.31–3.4/ 1.8–3.8	13/13	>30	0.15 × 0.22	>20	10

8. Challenges and future directions

The actual application and performance of microstrip dual-band bandpass filters in contemporary wireless systems are affected by a number of significant obstacles. One major obstacle among these is sensitivity to manufacturing tolerances and fabrication complexity. Particularly in filters incorporating linked resonators, dual-mode resonators, and stub-loaded resonators, precise control over resonator size and coupling is crucial. Due to parasitic effects and cross-coupling, such sensitivity might deteriorate filter performance, increasing the difficulty of the design and fabrication procedures. Even slight variations in resonator dimensions, substrate thickness, or dielectric characteristics can result in frequency shifts, degraded insertion loss, decreased isolation, and uneven return loss levels due to the compact and frequently complex geometries involved, such as coupled resonators, dual-mode resonators, and defected ground structures (DGS). In systems that demand great selectivity and sharp roll-offs, where exact control over coupling coefficients and transmission zeros is crucial, this manufacturing sensitivity is made worse. The electrical performance of the dual-band filter is impacted by these variances, which also make mass production more difficult because of lower yield and higher costs. Complexity is increased by the use of sophisticated materials and multi-layer structures, necessitating strict process controls.

Numerous solutions have been investigated to deal with these issues. In order to determine which design parameters are most susceptible to fabrication fluctuations, design procedures are increasingly using robust optimization techniques and tolerance analysis during the simulation phase. Potential performance loss can be predicted and mitigated by using Monte Carlo simulations and parameter sweeps. Additionally, using resonator architectures that are less sensitive to dimensional changes, like folded resonators or specific fractal geometries, can improve fabrication robustness. Additionally, the choice of materials is crucial. Temperature variations and manufacturing irregularities are lessened by low-loss, thermally stable substrates with precisely regulated dielectric constants. Higher resolution photolithography and exact etching procedures are examples of advanced fabrication techniques that increase dimensional accuracy, which improves filter performance and repeatability.

Adding tunability using MEMS, varactor diodes, or reconfigurable metamaterial components is another intriguing approach. Even with small dimensional errors, such adjustable components can correct for post-production frequency changes caused by fabrication, allowing for dynamic passband adjustment and design target restoration. In the future, combining dual-band filters with intelligent monitoring and adaptive control circuits may offer real-time compensation against fabrication and environmental variations, enhancing filter performance and dependability even more. As the next generation of dual-band BPFs must incorporate intricate electromagnetic design, precision fabrication processes, and nonlinear component integration, interdisciplinary collaboration will become more crucial to addressing these issues. Innovation and commercial adoption will also be accelerated by standardizing design procedures and performance indicators. It is anticipated that future developments will concentrate on improving reconfigurability and power handling capabilities, expanding stopband width without sacrificing insertion loss, and strengthening harmonic suppression. As demonstrated by new research trends and device implementations, such advancements will greatly assist a variety of applications, such as wireless communication, radar systems, and biomedical sensing. To address the demanding requirements of current and future wireless communication systems, a synergistic strategy integrating robust design, accurate manufacturing, adaptive tuning, and innovative materials is required.

Conventional microstrip filter topologies are facing more difficulties as wireless communication systems go toward millimeter-wave and sub-terahertz frequencies. Resonator structures become more sensitive to fabrication tolerances due to their downsizing, and their performance deteriorates when conductor and dielectric losses increase. Higher frequency filter properties are also greatly impacted by radiation leakage, parasitic coupling, and packaging effects. Future studies should concentrate on low-loss materials, sophisticated manufacturing processes, and substitute technologies such SIW, gap-waveguide, and MMIC-based implementations in order to overcome these constraints. Compact, high-performance filters for next-generation 6G and beyond wireless systems are anticipated to be made easier by the incorporation of AI-assisted design and optimization techniques.

9. Conclusion

In this article, the recent advances and challenges of designing dual-band bandpass filters have been reviewed. Different topologies and structures for the dual-band filters have been revealed, highlighting their advantages and limitations. While designing the dual-band filters, the designers are facing different challenges such as achieving wide bandwidth and high selectivity simultaneously, ensuring wide tuning range and fast response times, minimizing insertion losses, maintaining temperature stability, managing fabrication complexity, integrating filters into larger systems, handling high power levels, and establishing standardization in design and performance metrics. Addressing these challenges requires interdisciplinary collaboration, advancements in materials and fabrication techniques, and standardized testing procedures. Despite these obstacles, ongoing research and development efforts aim to drive further progress in dual-band filter technology for various applications in wireless communication, radar, and sensing systems. Novel materials like metamaterials and graphene, along with advanced tuning mechanisms such as varactor diodes and MEMS, have enabled the development of compact filters with enhanced dual-band functionality. These advancements promise to enhance wireless communication, radar, and sensing applications, with ongoing research expected to further drive innovation in the field.

Author contributions

Conceptualization, T.K.D., S.C. and B.G.; Methodology, T.K.D. and S.C.; Validation, S.C. and B.G.; Formal Analysis, T.K.D.; Investigation, T.K.D.; Resources, T.K.D., S.C. and B.G.; Data Curation, T.K.D.; Writing—Original Draft Preparation, T.K.D.; Writing—Review & Editing, S.C. and B.G.; Visualization, T.K.D.; Supervision, S.C. and B.G.; Project Administration, T.K.D. and S.C.

Conflict of interest

The authors declare no competing financial interest.

References

[1] V. Crnojević-Bengin, *Advances in Multi-Band Microstrip Filters*, 1st ed. Cambridge, U.K.: Cambridge University Press, 2015. https://doi.org/10.1017/CBO9781139976763.

[2] H. Miyake, S. Kitazawa, T. Ishizaki, T. Yamada, and Y. Nagatomi, "A miniaturized monolithic band filter using ceramic lamination technique for dual mode portable telephones," In Proc. 1997 IEEE MTT-S International Microwave Symposium Digest, Denver, CO, USA, Jun. 8-13, 1997, pp. 789-792. https://doi.org/10.1109/MWSYM.1997.602908.

[3] S. S. Maragheh, M. Dousti, M. Dolatshahi, and B. Ghalamkari, "Tunable dual-band bandpass filter for multi-standard applications," *AEU-International Journal of Electronics and Communications*, vol. 111, p. 152885, 2019. https://doi.org/10.1016/j.aeue.2019.152885.

[4] A. Lalbakhsh, S. M. Alizadeh, A. Ghaderi, A. Golestanifar, B. Mohamadzade, M. Jamshidi, and W. Mohyuddin, "A design of a dual-band bandpass filter based on modal analysis for modern communication systems," *Electronics*, vol. 9, no. 11, p. 1770, 2020. https://doi.org/10.3390/electronics9111770.

[5] W.-L. Hsu, P.-Y. Lyu, and S.-F. Chang, "Design of a miniature dual-band bandpass filter with interlocked stepped-impedance resonators for 5G new radio access technology," *International Journal of Microwave and Wireless Technologies*, vol. 12, no. 8, pp. 733-737, 2020. https://doi.org/10.1017/S1759078720001026.

[6] A. Lalbakhsh, A.Ghaderi, W.Mohyuddin, R.B. Simorangkir, N. Bayat-Makou, M.S. Ahmad, G.H. Lee, and K.W. Kim, "A compact C-band bandpass filter with an adjustable dual-band suitable for satellite communication systems," *Electronics*, vol. 9, no. 7, p.1088, 2020. https://doi.org/10.3390/electronics9071088.

[7] N. Claus, K. Y. Kapusuz, J. Verhaevert, and H. Rogier, "Compact and hybrid dual-band bandpass filter using folded multimode resonators and second-mode suppression," *Electronics*, vol. 13, no. 10, p. 1921, 2024. https://doi.org/10.3390/electronics13101921.

[8] W. Cheng, K. Deng, and W. Cheng, "Design of micro-strip symmetrical dual-band filter based on wireless sensor network nodes," *EURASIP Journal on Wireless Communications and Networking*, vol. 34, pp. 1-8, 2019. https://doi.org/10.1186/s13638-019-1347-y.

[9] S. Yıldız, A. Aksen, and S. B. Yarman, "Dual band filter design using real frequency technique and frequency transformation," *IU-Journal of Electrical and Electronics Engineering*, vol. 17, no. 2, pp. 3343-3350, 2017.

[10] T. A. M. Balde, F. Manene, and F. M. Mbango, "A dualband bandpass filter with tunable bandwidths for automotive radar and 5G millimeter-wave applications," *Indonesian Journal of Electrical Engineering and Computer Science*, vol. 27, no. 1, pp. 309-317, 2022. https://doi.org/10.11591/ijeecs.v27.i1.pp309-317.

[11] E. C. Britto, S. C. Xavier, and S. K. Danasegaran, "Design of narrowband terahertz filtenna for high-speed wireless communication," *Brazilian Journal of Physics*, vol. 54, pp. 1-17, 2024. https://doi.org/10.1007/s13538-024-01485-z.

[12] L. Gu and Y. Dong, "Compact dual-band bandpass filter with high selectivity based on spiral-stub-loaded dual-mode QMSIW resonators," *Microwave and Optical Technology Letters*, vol. 65, no. 2, pp. 559-566, 2023. https://doi.org/10.1002/mop.33541.

[13] J. Ge and G. Wang, "A dual-band filtering structure for highly selective reconfigurable bandpass filter and filtering balun," *International Journal of RF and Microwave Computer-Aided Engineering*, vol. 32, no. 8, p. e23215, 2022. https://doi.org/10.1002/mmce.23215.

[14] A. Arora, A. Madan, M. Bhattacharjee, C. Nayak, K. V. P. Kumar, and R. R. Thipparaju, "Implementation of a compact dual-band bandpass filter using signal interference technique on paper substrate," *AEU-International Journal of Electronics and Communications*, vol. 123, p. 153262, 2020. https://doi.org/10.1016/j.aeue.2020.153262.

[15] G. Macchiarella and S. Tamiazzo, "Design techniques for dual-passband filters," *IEEE Transactions on Microwave Theory and Techniques*, vol. 53, pp. 3265-3271, 2005. https://doi.org/10.1109/TMTT.2005.855749.

[16] P. Lenoir, S. Bila, F. Seyfert, D. Baillargeat, and S. Verdeyme, "Synthesis and design of asymmetrical dual-band bandpass filters based on equivalent network simplification," *IEEE Transactions on Microwave Theory and Techniques*, vol. 54, pp. 3090-3097, 2006. https://doi.org/10.1109/TMTT.2006.877037.

[17] X. Guan, Z. Ma, P. Cai, Y. Kobayashi, T. Anada, and G. Hagiwara, "Synthesis of dual-band bandpass filters using successive frequency transformations and circuit conversions," *IEEE Microwave and Wireless Components Letters*, vol. 16, pp. 110-112, 2006. https://doi.org/10.1109/LMWC.2006.869868.

[18] J. Lee and K. Sarabandi, "A synthesis method for dual-passband microwave filters," *IEEE Transactions on Microwave Theory and Techniques*, vol. 55, pp. 1163-1170, 2007. https://doi.org/10.1109/TMTT.2007.897712.

[19] G. Chaudhary, Y. Jeong, K. Kim, and D. Ahn, "Design of dual-band bandpass filters with controllable bandwidths using new mapping function," *Progress in Electromagnetics Research*, vol. 124, pp. 17-34, 2012. https://doi.org/10.2528/PIER11111407.

[20] Y.-T. Kuo and C.-Y. Chang, "Analytical design of two-mode dual-band filters using E-shaped resonators," *IEEE Transactions on Microwave Theory and Techniques*, vol. 60, pp. 250-260, 2012. https://doi.org/10.1109/TMTT.2011.2176506.

[21] R. Zhang and L. Zhu, "Synthesis and design of wideband dual-band bandpass filters with controllable in-band ripple factor and dual-band isolation," *IEEE Transactions on Microwave Theory and Techniques*, vol. 61, pp. 1820-1828, 2013. https://doi.org/10.1109/TMTT.2013.2256145.

[22] R. Zhang, S. Luo, and L. Zhu, "Asymmetrical-response dual-band bandpass filters on $\lambda/8$ transmission lines with modified Richard's transformation," *IEEE Microwave and Wireless Components Letters*, vol. 24, pp. 680-682, 2014. https://doi.org/10.1109/LMWC.2014.2341034.

[23] Y. Wu, L. Cui, Z. Zhuang, W. Wang, and Y. Liu, "A simple planar dual-band bandpass filter with multiple transmission poles and zeros," *IEEE Transactions on Circuits and Systems II: Express Briefs*, vol. 65, pp. 56-60, 2017. https://doi.org/10.1109/TCSII.2017.2702191.

[24] E. Z. C. Pheng and P. W. Wong, "Design and synthesis of dual-band microwave bandpass filter based on hybrid polynomials," *Progress in Electromagnetics Research C*, vol. 72, pp. 141-149, 2017. https://doi.org/10.2528/PIERC17012603.

[25] T. Lim, J. Ha, S. Lee, and Y. Lee, "Design method for dual-band filters with completely independent passbands," *Journal of Electromagnetic Waves and Applications*, vol. 33, pp. 1735-1748, 2019. https://doi.org/10.1080/09205071.2019.1636720.

[26] S. C. Tang, P. C. Chu, J. T. Kuo, and L. K. Wu, "Dual-band bandpass filter based on frequency transformations with enhanced inter-band isolation," In Proc. 2020 IEEE Asia-Pacific Microwave Conference, Hong Kong, Dec. 8-11, 2020, pp. 758-760. https://doi.org/10.1109/APMC47863.2020.9331380.

[27] X. Dai, Q. Yang, H. Du, C. Guo, and A. Zhang, "Direct synthesis method for dual-band bandpass filters with wide fractional bandwidth range and center frequency ratio," *IEEE Transactions on Circuits and Systems II: Express Briefs*, vol. 68, pp. 2755-2759 2021. https://doi.org/10.1109/TCSII.2021.3063731.

[28] R. Gomez-Garcia and M. Sanchez-Renedo, "Single- and dual-passband microwave planar filters with coupled double-transmission-line resonators," *IET Microwaves, Antennas and Propagation*, vol. 3, no. 6, pp. 917-928, 2009. https://doi.org/10.1049/IET-MAP.2008.0292.

[29] J. T. Kuo, C. Y. Fan, and S. C. Tang, "Dual-wideband bandpass filters with extended stopband based on coupled-line and coupled three-line resonators," *Progress in Electromagnetics Research*, vol. 124, pp. 1-15, 2012. https://doi.org/10.2528/PIER11120103.

[30] S. Zhang and L. Zhu, "Compact split-type dual-band bandpass filter based on $\lambda/4$ resonators," *IEEE Microwave and Wireless Components Letters*, vol. 23, pp. 344-346, 2013. https://doi.org/10.1109/LMWC.2013.2264659.

[31] M. Makimoto and S. Yamashita, "Bandpass filters using parallel coupled stripline stepped impedance resonators," *IEEE Transactions on Microwave Theory and Techniques*, vol. 28, pp. 1413-1417, 1980. https://doi.org/10.1109/TMTT.1980.1130258.

[32] Y. P. Zhang and M. Sun, "Dual-band microstrip bandpass filter using stepped-impedance resonators with new coupling schemes," *IEEE Transactions on Microwave Theory and Techniques*, vol. 54, pp. 3779-3785, 2006. https://doi.org/10.1109/TMTT.2006.882895.

[33] M. A. S. Alkanhal, "Dual-band bandpass filters using inverted stepped-impedance resonators," *Journal of Electromagnetic Waves and Applications*, vol. 23, no. 8-9, pp. 1211-1220, 2009. https://doi.org/10.1163/156939309789023411.

[34] X. Y. Zhang, C. H. Chan, Q. Xue, and B. J. Hu, "Dual-band bandpass filter with controllable bandwidths using two coupling paths," *IEEE Microwave and Wireless Components Letters*, vol. 20, pp. 616-618, 2010. https://doi.org/10.1109/LMWC.2010.2066553.

[35] C. H. Kim and K. Chang, "Independently controllable dual-band bandpass filters using asymmetric stepped-impedance resonators," *IEEE Transactions on Microwave Theory and Techniques*, vol. 59, pp. 3037-3047, 2011. https://doi.org/10.1109/TMTT.2011.2168973.

[36] J. Marimuthu, A. M. Abbosh, and B. Henin, "Planar microstrip bandpass filter with wide dual bands using parallel-coupled lines and stepped impedance resonators," *Progress in Electromagnetics Research C*, vol. 35, pp. 49-61, 2013. https://doi.org/10.2528/PIERC12110402.

[37] E. S. Ahmaed, "Compact dual-band parallel coupled T-shaped SIR filter for WLAN applications," *TELKOMNIKA (Telecommunication Computing Electronics and Control)*, vol. 15, no. 4, pp. 1677-1681, 2017. https://doi.org/10.12928/TELKOMNIKA.v15i4.5584.

[38] G. Sung, "Compact dual-band bandpass filter using U-shaped stepped-impedance resonators with parallel coupled structures," *Journal of Electromagnetic Engineering and Science*, vol. 18, no. 2, pp. 73-77, 2018. https://doi.org/10.26866/jees.2018.18.2.73.

[39] D. Li, J. A. Wang, Y. Liu, Z. Chen, and L. Yang, "Selectivity-enhancement technique for parallel-coupled SIR based dual-band bandpass filter," *Microwave and Optical Technology Letters*, vol. 63, pp. 787-792, 2021. https://doi.org/10.1002/mop.32672.

[40] M. Firmli and A. Zatni, "Dual-wideband sandwich coupled three-lines bandpass filter based on modified open-stub loaded stepped impedance resonator with improved second harmonic for 5G wi-fi/ku-band applications," *Heliyon*, vol. 9, no. 2, pp. 1-13, 2023. https://doi.org/10.1016/j.heliyon.2023.e13365.

[41] J. T. Kuo and H. P. Lin, "Dual-band bandpass filter with improved performance in extended upper rejection band," *IEEE Transactions on Microwave Theory and Techniques*, vol. 57, pp. 824-829, 2009. https://doi.org/10.1109/TMTT.2009.2015040.

[42] S. C. Lin and T. L. Jong, "Microstrip bandpass filters with various resonators using connected- and edge-coupling mechanisms and their applications to dual-band filters and diplexers," *IEEE Transactions on Microwave Theory and Techniques*, vol. 60, pp. 975-988, 2012. https://doi.org/10.1109/TMTT.2012.2183380.

[43] L. Yang, W. W. Choi, K. W. Tam, and L. Zhu, "Balanced dual-band bandpass filter with multiple transmission zeros using doubly short-ended resonator coupled line," *IEEE Transactions on Microwave Theory and Techniques*, vol. 63, pp. 2225-2232, 2015. https://doi.org/10.1109/TMTT.2015.2431679.

[44] H. Zhu and A. M. Abbosh, "Single- and dual-band bandpass filters using coupled stepped-impedance resonators with embedded coupled-lines," *IEEE Microwave and Wireless Components Letters*, vol. 26, no. 9, pp. 675-677, 2016. https://doi.org/10.1109/LMWC.2016.2597180.

[45] N. Kumar and Y. K. Singh, "Single/dual-band BPFs with spurious band suppression by using non-uniform coupled resonators," *Progress in Electromagnetics Research C*, vol. 66, pp. 63-76, 2016. https://doi.org/10.2528/PIERC16030206.

[46] M. H. Weng, S. W. Lan, S. J. Chang, and R. Y. Yang, "Design of dual-band bandpass filter with simultaneous narrow- and wide-bandwidth and a wide stopband," *IEEE Access*, vol. 7, pp. 147694-147703, 2019. https://doi.org/10.1109/ACCESS.2019.2946302.

[47] S. Chaimool and P. Akkaraekthalin, "Resonator-embedded four-pole cross-coupled dual-band microstrip bandpass filters," In Proc. 2006 International Symposium on Communications and Information Technologies, Bangkok, Thailand, Oct. 18-20, 2006, pp. 1076-1079. https://doi.org/10.1109/ISCIT.2006.339943.

[48] J. W. Fan, C. H. Liang, and B. Wu, "Cross-coupled dual-band filter using folded tri-section stepped impedance resonators," *Microwave and Optical Technology Letters*, vol. 50, no. 2, pp. 407-409, 2008. https://doi.org/10.1002/mop.23110.

[49] B. Wu, C. H. Liang, Q. Li, and P. Y. Qin, "Novel dual-band filter incorporating defected SIR and microstrip SIR," *IEEE Microwave and Wireless Components Letters*, vol. 18, pp. 392-394, 2008. https://doi.org/10.1109/LMWC.2008.922614.

[50] W.-J. Lin, C.-S. Chang, J.-Y. Li, D.-B. Lin, L.-S. Chen, and M.-P. Houng, "A new approach of dual-band filters by stepped impedance simplified cascaded quadruplet resonators with slot coupling," *Progress in Electromagnetics Research Letters*, vol. 9, pp. 19-28, 2009. https://doi.org/10.2528/PIERL09042801.

[51] J. Li, C. Chen, and W. Wu, "Design of dual-passband cross-coupled filter using stub-loaded open-loop resonators," In Proc. 2009 Asia Pacific Microwave Conference, Singapore, Dec. 7-10, 2009, pp. 929-932. https://doi.org/10.1109/APMC.2009.5384320.

[52] M. H. Weng, C. H. Kao, and Y. C. Chang, "A compact dual-band bandpass filter with high band selectivity using cross-coupled asymmetric SIRs for WLANs," *Journal of Electromagnetic Waves and Applications*, vol. 24, pp. 161-168, 2010. https://doi.org/10.1163/156939310790735679.

[53] R. Y. Yang, C. Y. Hung, and J. S. Lin, "A dual-band bandpass filter with an enhanced second passband performance using modifiable coupling," *Journal of Electromagnetic Waves and Applications*, vol. 25, no. 2-3, pp. 305-314, 2011. https://doi.org/10.1163/156939311794362803.

[54] X. Chen, L. Li, Y. Zhang, Y. Geng, and W. Zhang, "Balanced dual-band bandpass filter based on asymmetrical coupled lines," *Electromagnetics*, vol. 32, no. 1, pp. 1-7, 2012. https://doi.org/10.1080/02726343.2012.633875.

[55] Z. J. Su, X. Chen, L. Li, B. Wu, and C.-H. Liang, "A folded SIR cross coupled WLAN dual-band filter," *Progress in Electromagnetics Research Letters*, vol. 45, pp. 115-119, 2014. https://doi.org/10.2528/PIERL14032502.

[56] L. Lin, Z. Zhang, S. J. Sun, and C.-H. Liang, "Dual-band bandpass filter with wide upper stopband using novel stepped impedance stub-loaded quad-mode resonator," *Progress in Electromagnetics Research Letters*, vol. 51, pp. 61-66, 2015. https://doi.org/10.2528/PIERL14120601.

[57] J. W. Eun and J.-H. Lee, "A microstrip dual-band bandpass filter using feed line with SIR," *IEICE Electronics Express*, vol. 14, no. 4, p. 20170022, 2017. https://doi.org/10.1587/elex.14.20170022.

[58] N. Wattikornsirikul, J. Konpang, S. Tubtongdee, and A. Sirikham, "High-selectivity dual-band bandpass filter by utilizing asymmetrical stepped-impedance resonator," *UTK Research Journal*, vol. 14, pp. 10-18, 2020.

[59] C.-H. Lee, Y.-H. Hsieh, and M.-H. Ho, "Design of compact dual-band bandpass filters using $\lambda/2$ and combined $\lambda/4$ stepped-impedance resonators," *Microwave and Optical Technology Letters*, vol. 49, no. 1, pp. 2703-2706, 2007. https://doi.org/10.1002/mop.22823.

[60] Y.-H. Hsieh, C.-H. Lee, and C.-I.-G. Hsu, "Design of spur-line-loaded cross-coupled dual-band bandpass filter with wide upper-end stopband," *Microwave and Optical Technology Letters*, vol. 50, no. 3. pp. 691-694, 2008. https://doi.org/10.1002/mop.23186.

[61] Y.-C. Chang, C.-H. Kao, M.H. Weng, and R.-Y. Yang, "Design of the compact dual-band bandpass filter with high isolation for GPS/WLAN applications," *IEEE Microwave and Wireless Components Letters*, vol. 19, no. 12, pp. 780-782, 2009. https://doi.org/10.1109/LMWC.2009.2033499.

[62] P.-H. Deng and H.-H. Tung, "Design of microstrip dual-passband filter based on branch-line resonators," *IEEE Microwave and Wireless Components Letters*, vol. 21, no. 4, pp. 200-202, 2011. https://doi.org/10.1109/LMWC.2011.2105257.

[63] F.-C. Chen and Q.-X. Chu, "Design of dual-band CT filter with source load coupling," *Journal of Electromagnetic Waves and Applications*, vol. 25, no. 1, pp. 15-22, 2011. https://doi.org/10.1163/156939311793898332.

[64] B. Wang, X. H. Wang, B. Z. Wang, and H. Zhang, "Compact microstrip dual-band bandpass filter with multiple transmission zeros," *Journal of Electromagnetic Waves and Applications*, vol. 27, no. 7, pp. 930-937, 2013. https://doi.org/10.1080/09205071.2013.792751.

[65] M. Hayati and A. Khajavi, "A dual-band bandpass filter using coupled semi-circular stepped impedance resonators with sharp roll-off and wide stopband," *Arabian Journal for Science and Engineering*, vol. 39, pp. 3963-3968, 2014. https://doi.org/10.1007/s13369-014-1017-7.

[66] M.-H. Weng, S. Wu, S.-B. Jhong, Y.-C. Chang, and M.-S. Lee, "A novel compact dual-mode filter using cross-slotted patch resonator for dual-band applications," In Proc. 2007 IEEE/MTT-S International Microwave Symposium, Honolulu, HI, USA, Jun. 3-8, 2007, pp. 921-924. https://doi.org/10.1109/MWSYM.2007.380131.

[67] S. Luo and L. Zhu, "A novel dual-mode dual-band bandpass filter based on a single ring resonator," *IEEE Microwave and Wireless Components Letters*, vol. 19, no. 8, pp. 497-499, 2009. https://doi.org/10.1109/LMWC.2009.2024826.

[68] S. Luo, L. Zhu, and S. Sun, "A dual-band ring-resonator bandpass filter based on two pairs of degenerate modes," *IEEE Transactions on Microwave Theory and Techniques*, vol. 58, no. 12, pp. 3427-3423, 2010. https://doi.org/10.1109/TMTT.2010.2053590.

[69] Y. Sung, "Dual-mode dual-band filter with band notch structures," *IEEE Microwave and Wireless Components Letters*, vol. 20, no. 2, pp. 73-75, 2010. https://doi.org/10.1109/LMWC.2009.2038434.

[70] Y. Li, H. Wong, and Q. Xue, "Dual-mode dual-band bandpass filter based on a stub-loaded patch resonator," *IEEE Microwave and Wireless Components Letters*, vol. 21, no. 10, pp. 525-527, 2011. https://doi.org/10.1109/LMWC.2011.2164394.

[71] S. Fu, B. Wu, J. Chen, S. Sun, and C. Liang, "Novel second-order dual-mode dual-band filters using capacitance loaded square loop resonator," *IEEE Transactions on Microwave Theory and Techniques*, vol. 60, no. 3, pp. 477-483, 2012. https://doi.org/10.1109/TMTT.2011.2181859.

[72] R. Zhang, L. Zhu, and S. Luo, "Dual-mode dual-band bandpass filter using a single slotted circular patch resonator," *IEEE Microwave and Wireless Components Letters*, vol. 22, no. 5, pp. 233-235, 2012. https://doi.org/10.1109/LMWC.2012.2192419.

[73] C. Karpuz and A. K. Gorur, "A novel compact configuration for dual-mode microstrip resonators and dual-band bandpass filter applications," *Microwave and Optical Technology Letters*, vol. 55, pp. 775-779, 2013. https://doi.org/10.1002/mop.27444.

[74] C. Karpuz, A. K. Gorur, and E. Sahin, "Dual-mode dual-band microstrip bandpass filter with controllable center frequency," *Microwave and Optical Technology Letters*, vol. 57, no. 3, pp. 639-642, 2015. https://doi.org/10.1002/mop.28914.

[75] S. Sun, "A dual-band bandpass filter using a single dual-mode ring resonator," *IEEE Microwave and Wireless Components Letters*, vol. 21, pp. 298-300, 2011. https://doi.org/10.1109/LMWC.2011.2132119.

[76] D. Li, J.-A. Wang, Y. Liu, and Z. Chen, "Miniaturized dual-band bandpass filter with sharp roll-off using ring-loaded resonator," *IEEE Access*, vol. 8, pp. 25588-25595, 2019. https://doi.org/10.1109/ACCESS.2019.2958390.

[77] M.-H. Weng, H.W. Wu, and Y.-K. Su, "Compact and low loss dual-band bandpass filter using pseudo-interdigital stepped impedance resonators for WLANs," *IEEE Microwave and Wireless Components Letters*, vol. 17, no. 3, pp. 187-189, 2007. https://doi.org/10.1109/LMWC.2006.890463.

[78] Q.-X. Chu and F.-C. Chen, "A compact dual-band bandpass filter using meandering stepped impedance resonators," *IEEE Microwave and Wireless Components Letters*, vol. 18, pp. 320-322, 2008. https://doi.org/10.1109/LMWC.2008.922117.

[79] L. Guo, Y. Zhi-Yuan, and L. Zhang, "Design of a dual-mode dual-band filter using stepped impedance resonators," *Progress in Electromagnetics Research Letters*, vol. 14, pp. 147-154, 2010. https://doi.org/10.2528/PIERL10032601.

[80] H.-J. Yuan and Y. Fan, "Compact microstrip dual-band filter with stepped-impedance resonators," *IET Electronics Letters*, vol. 47, no. 44, pp. 1328, 2011. https://doi.org/10.1049/el.2011.2671.

[81] H.-W. Deng, Y.-J. Zhao, X.-S. Zhang, W. Chen, and J.-K. Wang, "Compact and high selectivity dual-band dual-mode microstrip BPF with single stepped-impedance resonator," *IET Electronics Letters*, vol. 47, no. 5, pp. 326-327, 2011. https://doi.org/10.1049/el.2011.0054.

[82] Z. Yao, C. Wang, and N. Y. Kim, "A compact dual-mode dual-band bandpass filter using stepped-impedance open-loop resonators and center-loaded resonators," *Microwave and Optical Technology Letters*, vol. 55, pp. 3000-3005, 2013. https://doi.org/10.1002/mop.27952.

[83] S. Yang, L. Lin, J. Chen, K. Deng, and C. H. Liang, "Design of compact dual-band bandpass filter using dual-mode stepped-impedance stub resonators," *IET Electronics Letters*, vol. 50, no. 8, pp. 611-613, 2014. https://doi.org/10.1049/el.2013.4217.

[84] C.-F. Chen, S.-F. Chang, B.-H. Tseng, and J.-H. Weng, "Compact dual-band stepped-impedance resonator filter with separate coupling paths," *IET Electronics Letters*, vol. 50, no. 21, pp. 1551-1552, 2014. https://doi.org/10.1049/el.2014.2982.

[85] H. Lu, J. Huang, X. Zhang, N. Yuan, and Z. Huang, "Dual-mode dual-band microstrip bandpass filter based on stepped impedance resonator (SIR) for wireless communication applications," In Proc. 2016 International Conference on Communication and Electronic Information Engineering, Guangzhou, China, Oct. 15-16, 2016, pp. 758-764. https://doi.org/10.2991/ceie-16.2017.98.

[86] K. Deng, Z. Chen, G. Hu, and W. Feng, "Dual-band bandpass filters with multiple transmission zeros using $\lambda/4$ stepped-impedance resonators," *International Journal of RF and Microwave Computer-Aided Engineering*, vol. 29, p. e21469, 2019. https://doi.org/10.1002/mmce.21469.

[87] A. M. Moattari, A. Bijari, and S. M. Razavi, "A new compact microstrip dual bandpass filter using stepped impedance and $\lambda/2$ bended resonators," *International Journal of RF and Microwave Computer-Aided Engineering*, vol. 31, p. e22568, 2021. https://doi.org/10.1002/mmce.22568.

[88] C.-W. Tang and P.-H. Wu, "Design of a planar dual-band bandpass filter," *IEEE Microwave and Wireless Components Letters*, vol. 21, no. 7, pp. 362-364, 2011. https://doi.org/10.1109/LMWC.2011.2151849.

[89] M. Hayati, L. Noori, and A. Adinehvand, "Compact dual-band bandpass filter using open loop resonator for multimode WLANs," *IET Electronics Letters*, vol. 48, no. 10, pp. 573-574, 2012. https://doi.org/10.1049/el.2012.0439.

[90] J. Shi, L. Lin, J. X. Chen, H. Chu, and X. Wu, "Dual-band bandpass filter with wide stopband using one stepped-impedance ring resonator with shorted stubs," *IEEE Microwave and Wireless Components Letters*, vol. 24, no. 7, pp. 442-444, 2014. https://doi.org/10.1109/LMWC.2014.2316259.

[91] X. Y. Zhang, J.-X. Chen, Q. Xue, and S.-M. Li, "Dual-band bandpass filters using stub-loaded resonators," *IEEE Microwave and Wireless Components Letters*, vol. 17, no. 8, pp. 583-585, 2007. https://doi.org/10.1109/LMWC.2007.901768.

[92] P. Mondal and M. Mandal, "Design of dual-band bandpass filters using stub-loaded open loop resonators," *IEEE Transactions on Microwave Theory and Techniques*, vol. 56, pp. 150-155, 2008. https://doi.org/10.1109/TMTT.2007.912204.

[93] X. Wu, F. Wan, and J. Ge, "Stub-loaded theory and its application to balanced dual-band bandpass filter design," *IEEE Microwave and Wireless Components Letters*, vol. 26, no. 4, pp. 231-233, 2017. https://doi.org/10.1109/LMWC.2016.2537045.

[94] G.-Z. Liang and F.-C. Chen, "A compact dual-wideband bandpass filter based on open-/short-circuited stubs," *IEEE Access*, vol. 8, pp. 20488-20492, 2020. https://doi.org/10.1109/ACCESS.2020.2968518.

[95] M. Zhou, X. Tang, and F. Xiao, "Compact dual band bandpass filter using novel E-type resonators with controllable bandwidths," *IEEE Microwave and Wireless Components Letters*, vol. 18, no. 12, pp. 779-781, 2008. https://doi.org/10.1109/LMWC.2008.2007696.

[96] J. Xu and W. Wu, "Compact microstrip dual-mode dual-band bandpass filters using stubs loaded coupled line," *Progress in Electromagnetics Research C*, vol. 41, pp. 137-150, 2013. https://doi.org/10.2528/PIERC13052204.

[97] Z.-C. Zhang, Q.-X. Chu, and F.-C. Chen, "Compact dual-band bandpass filters using open-/short-circuited stub-loaded $\lambda/4$ resonators," *IEEE Microwave and Wireless Components Letters*, vol. 25, no. 10, pp. 657-659, 2015. https://doi.org/10.1109/LMWC.2015.2463216.

[98] M. Á. Sánchez-Soriano and R. Gómez-García, "Sharp-rejection wide-band dual-band bandpass planar filters with broadly-separated passbands," *IEEE Microwave and Wireless Components Letters*, vol. 25, pp. 97-99, 2014. https://doi.org/10.1109/LMWC.2014.2382669.

[99] O. Abu Safia, M. Nedil, M. C. Yagoub, L. Talbi, and K. Hettak, "Compact dual-band bandpass filters with stub resonating lines," *Microwave and Optical Technology Letters*, vol. 59, no. 7, pp. 1619-1625, 2017. https://doi.org/10.1002/mop.30593.

[100] M. Sun, Z. Chen, T. Zuo, Z. Zuo, and A. Zhang, "A high selectivity dual-band bandpass filter using quadruple-mode multi-stub loaded ring resonator (SLRR)," *International Journal of RF and Microwave Computer-Aided Engineering*, vol. 31, p. e22667, 2021. https://doi.org/10.1002/mmce.22667.

[101] Y. X. Wang, Y. L. Chen, W. H. Zhou, W. C. Yang, and J. Zen, "Dual-band bandpass filter design using stub-loaded hairpin resonator and meandering uniform impedance resonator," *Progress in Electromagnetics Research Letters*, vol. 95, pp. 147-153, 2021. https://doi.org/10.2528/PIERL20102102.

[102] Y. Xie, F. C. Chen, and Z. Li, "Design of dual-band bandpass filter with high isolation and wide stopband," *IEEE Access*, vol. 5, pp. 25602-25608, 2017. https://doi.org/10.1109/ACCESS.2017.2773502.

[103] Y. Xiong, L. T. Wang, W. Zhang, F. Zhang, D. Pang, M. He, X. Zhao, and L. Ji, "Design of dual band bandpass filter with closely spaced passbands and multiple transmission zeros," *Progress in Electromagnetics Research Letters*, vol. 70, pp. 45-51, 2017. https://doi.org/10.2528/PIERL17062801.

[104] J. M. Yan, B. J. Kang, Y. Yang, and L. Cao, "Single- and dual-band bandpass filters based on a novel microstrip loop-type resonators loaded with shorted stubs," *Progress in Electromagnetics Research Letters*, vol. 113, pp. 61-67, 2023. https://doi.org/10.2528/PIERL23083105.

[105] X. Y. Zhang, J. X. Chen, J. Shi, and Q. Xue, "High-selectivity dual-band bandpass filter using asymmetric stepped-impedance resonators," *IET Electronics Letters*, vol. 45, pp. 63-64, 2009. https://doi.org/10.1049/el:20091939.

[106] M. Z. Du, J.-X. Chen, Y.-J. Yang, and Z. H. Bao, "Balanced dual-band bandpass filter using stub-loaded stepped-impedance resonators," *Journal of Electromagnetic Waves and Applications*, vol. 27, pp. 2056-2064, 2013. https://doi.org/10.1080/09205071.2013.831740.

[107] A. J. Alazemi, "Dual-band and wideband bandpass filters using coupled lines and tri-stepped impedance stubs," *Micromachines*, vol. 14, no. 6, p. 1254, 2023. https://doi.org/10.3390/mi14061254.

[108] F.-C. Chen and Q.-X. Chu, "Novel multistub loaded resonator and its application to high-order dual-band filters," *IEEE Transactions on Microwave Theory and Techniques*, vol. 58, no. 6, pp. 1551-1556, 2010. https://doi.org/10.1109/TMTT.2010.2049161.

[109] G. Y. Wei, Y. X. Wang, J. Liu, and H. P. Li, "Design of a planar compact dual-band bandpass filter with multiple transmission zeros using a stub-loaded structure," *Progress in Electromagnetics Research Letters*, vol. 109, pp. 23-30, 2023. https://doi.org/10.2528/PIERL22122603.

[110] P. Jarry and J. Beneat, *Design and Realization of Miniaturized Fractal RF and Microwave Filters*. New Jersey: Wiley, 2009.

[111] F. Talaei, M. N. Azarmanesh, G. Askari, and H. Mirmohammadsadeghi, "A novel dual-mode dual band bandpass filter using a quasi-fractal structure," *IEICE Electronics Express*, vol. 7, pp. 153-158, 2010. https://doi.org/10.1587/elex.7.153.

[112] J. C. Liu, H. H. Liu, K. D. Yeh, C. Y. Liu, B. H. Zeng, and C. C. Chen, "Miniaturized dual-mode resonators with Minkowski-island-based fractal patch for WLAN dual-band systems," *Progress in Electromagnetics Research C*, vol. 26, pp. 229-243, 2012. https://doi.org/10.2528/PIERC11111502.

[113] H. T. Ziboon and J. K. Ali, "Compact dual-band bandpass filter based on fractal stub-loaded resonator," in *Proc. 2017 Progress in Electromagnetics Research Symposium*, St. Petersburg, Russia, May 2017, pp. 1815-1819. https://doi.org/10.1109/PIERS.2017.8262046.

[114] H. S. Lu, Q. Li, J. J. Huang, X. F. Zhang, and N. C. Yuan, "Dual-mode dual-band microstrip bandpass filter with high selection performance," in *Proc. 2016 Progress in Electromagnetics Research Symposium*, Shanghai, China, Aug. 2016, pp. 3517-3522. https://doi.org/10.1109/PIERS.2016.7735361.

[115] Y. S. Mezaal, H. T. Eyyuboglu and J. K. Ali, "New Dual Band Dual-Mode Microstrip Patch Bandpass Filter Designs Based on Sierpinski Fractal Geometry," in *Proc. 2013 Third International Conference on Advanced Computing and Communication Technologies (ACCT)*, Rohtak, India, June 2013, pp. 348-352. https://doi.org/10.1109/ACCT.2013.55.

[116] H. S. Lu, J. Yan, Q. Li, J. J. Huang, X. F. Zhang, and N. C. Yuan, "Design of dual-mode dual-band microstrip bandpass filter based on Sierpinski fractal geometry," in *Proc. 2016 IEEE International Conference on Microwave and Millimeter Wave Technology*, Beijing, China, Jun. 2016, vol. 1, pp. 369-371. https://doi.org/10.1109/ICMMT.2016.7761778.

[117] B. Decoster, S. Maes, I. Cuiñas, M. García Sánchez, R. Caldeirinha, and J. Verhaevert, "Dual-band single-layer fractal frequency selective surface for 5G applications," *Electronics*, vol. 10, p. 2880, 2021. https://doi.org/10.3390/electronics10222880.

[118] E. S. Ahmed, "Dual-mode dual-band microstrip bandpass filter based on fourth iteration T-square fractal and shorting pin," *Radioengineering*, vol. 21, 2012. https://doi.org/10.13164/re.2021-2.

[119] V. Crnojević-Bengin, K. Zemlyakov, N. Janković, and I. Vendik, "Dual-band bandpass filters based on dual-mode Hilbert fractal resonator," *Microwave and Optical Technology Letters*, vol. 55, pp. 1440-1443, 2013. https://doi.org/10.1002/mop.27667.

[120] H. Wu, Y. Chen, and Y. Chen, "Multi-layered dual-band bandpass filter using stub-loaded stepped-impedance and uniform-impedance resonators," *IEEE Microwave and Wireless Components Letters*, vol. 22, pp. 114-116, 2012. https://doi.org/10.1109/LMWC.2012.2185784.

[121] B. Wu, C. Liang, P. Qin, and Q. Li, "Compact dual-band filter using defected stepped impedance resonator," *IEEE Microwave and Wireless Components Letters*, vol. 18, pp. 674-676, 2008. https://doi.org/10.1109/LMWC.2008.2003459.

[122] L. Ren and H. Huang, "Dual-band bandpass filter based on dual-plane microstrip/interdigital DGS slot structure," *IET Electronics Letters*, vol. 45, pp. 1077-1079, 2009. https://doi.org/10.1049/el.2009.1851.

[123] J. Chen, T. Yum, J. Li, and Q. Xue, "Dual-mode dual-band bandpass filter using stacked loop structure," *IEEE Microwave and Wireless Components Letters*, vol. 16, pp. 502-504, 2006. https://doi.org/10.1109/LMWC.2006.880705.

[124] G. Chaudhary, H. Choi, Y. Jeong, J. Lim, D. Kim, and J. C. Kim, "Design of dual-band bandpass filter using DGS with controllable second passband," *IEEE Microwave and Wireless Components Letters*, vol. 21, pp. 589-591, 2011. https://doi.org/10.1109/LMWC.2011.2167140.

[125] X. Cao, Z. Tang, F. Wang, Y. Wu, and B. Zhang, "A novel dual-band bandpass filter using CRLH triangle mushroom structure and DGS," *Microwave and Optical Technology Letters*, vol. 55, no. 11, pp. 2756-2759, 2013. https://doi.org/10.1002/mop.27940.

[126] Y. Li, H. C. Yang, and S.-Q. Xiao, "Design of dual band filter based on a novel DGS structure," *Progress in Electromagnetics Research Letters*, vol. 41, pp. 167-174, 2013. https://doi.org/10.2528/PIERL13061503.

[127] X. Jin, Z. H. Zhang, L. Wang, and B.-R. Guan, "Compact dual-band bandpass filter using single meander multimode DGS resonator," *IET Electronics Letters*, vol. 49, pp. 1083-1084, 2013. https://doi.org/10.1049/el.2013.0977.

[128] K. Song, F. Zhang, and Y. Fan, "Miniaturized dual-band bandpass filter with good frequency selectivity using SIR and DGS," *AEU-International Journal of Electronics and Communications*, vol. 68, no. 5, pp. 384-387, 2014. https://doi.org/10.1016/j.aeue.2013.10.005.

[129] L.-H. Zhou, Y.-L. Ma, J. Shi, J.-X. Chen, and W. Che, "Differential dual-band bandpass filter with tunable lower band using embedded DGS unit for common-mode suppression," *IEEE Transactions on Microwave Theory and Techniques*, vol. 64, no. 12, pp. 4183-4191, 2016. https://doi.org/10.1109/TMTT.2016.2607176.

[130] S. O. Coumar, "Miniaturized DGS based multi-band pass filters for satellite applications," *Journal of Ambient Intelligence and Humanized Computing*, vol. 13, pp. 241-249, 2022. https://doi.org/10.1007/s12652-021-02898-3.

[131] Y. Rao, H. J. Qian, B. Yang, R. Gómez-García, and X. Luo, "Dual-band bandpass filter and filtering power divider with ultra-wide upper stopband using hybrid microstrip/DGS dual-resonance cells," *IEEE Access*, vol. 8, pp. 23624-23637, 2020. https://doi.org/10.1109/ACCESS.2020.2970209.

[132] D. Girbau, A. Lázaro, E. Martínez, D. Masone, and L. Pradell, "Tunable dual-band bandpass filter for WLAN applications," *Microwave and Optical Technology Letters*, vol. 51, pp. 2025-2028, 2009. https://doi.org/10.1002/mop.24550.

[133] X. Huang, L. Zhu, Q. Feng, Q. Xiang, and D. Jia, "Tunable bandpass filter with independently controllable dual passbands," *IEEE Transactions on Microwave Theory and Techniques*, vol. 61, pp. 3200-3208, 2013. https://doi.org/10.1109/TMTT.2013.2273894.

[134] F. Liang, X. Zhai, W. Lu, Q. Wan, and Y. Zhang, "An independently tunable dual-band filter using asymmetric $\lambda/4$ resonator pairs with shared via-hole ground," *Progress in Electromagnetics Research*, vol. 146, pp. 99-108, 2014. https://doi.org/10.2528/PIER14032505.

[135] F. Liang, W. Cai, W. Lu, L. Deng, and X. Zhai, "An independently tunable dual-band bandpass filter using a center shorting-stub-loaded resonator," *Progress in Electromagnetics Research C*, vol. 67, pp. 31-40, 2016. https://doi.org/10.2528/PIERC16053102.

[136] M. Danaeian, E. Zarezadeh, and H. Ghayoumi-Zadeh, "A compact and high performance dual-band bandpass filter based on unbalanced composite right/left-handed transmission lines for WLANs applications," *Analog Integrated Circuits and Signal Processing*, vol. 94, pp. 469-479, 2018. https://doi.org/10.1007/s10470-018-1104-x.

[137] E. E. Djoumessi, M. Chaker, and K. Wu, "Varactor-tuned quarter-wavelength dual-bandpass filter," *IET Microwaves, Antennas and Propagation*, vol. 3, pp. 117-124, 2009. https://doi.org/10.1049/iet-map:20080040.

[138] G. Chaudhary, Y. Jeong, and J. Lim, "Harmonic suppressed dual-band bandpass filters with tunable passbands," *IEEE Transactions on Microwave Theory and Techniques*, vol. 60, no. 7, pp. 2115-2123, 2012. https://doi.org/10.1109/TMTT.2012.2197020.

[139] G. Chaudhary, Y. Jeong, and J. Lim, "Dual-band bandpass filter with independently tunable center frequencies and bandwidths," *IEEE Transactions on Microwave Theory and Techniques*, vol. 61, no. 1, pp. 107-116, 2012. https://doi.org/10.1109/TMTT.2012.2222910.

[140] E. Park, D. Lim, and S. Lim, "Dual-band band-pass filter with fixed low band and fluidically-tunable high band," *Sensors*, vol. 17, no. 8, p. 1884, 2017. https://doi.org/10.3390/s17081884.

[141] Z. Brito-Brito, I. Llamas-Garro, G. Navarro-Muñoz, J. Perruisseau-Carrier, L. Pradell, F. Giacomozzi, and S. Colpo, "Precise frequency and bandwidth control of switchable microstrip bandpass filters using diode and microelectro-mechanical system technologies," *IET Microwaves, Antennas and Propagation*, vol. 6, no. 6, pp. 713-719, 2012. https://doi.org/10.1049/iet-map.2012.0077.